Polymer 344 (2026) 129495

Contents lists available at ScienceDirect

Polymer

journal homepage: www.elsevier.com/locate/polymer

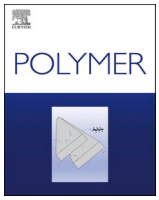

Investigating HDPE composites with phosphorus- and nitrogen-modified lignins

Alexander F. Tiniakos [a,*], Christina Samiotaki [b], Alexandra Zamboulis [b,**], Alexios Grigoropoulos [a], Stefania Koutsourea [a], Evangelia Tarani [c], Aikaterini Teknetzi [c], George Vourlias [c], Alexandros Zoikis Karathanasis [a], Dimitrios N. Bikiaris [b], Ioanna Deligkiozi [d]

[a] Creative Nano PC, 43 Tatoiou, Metamorfosi, 14451, Athens, Greece
[b] Laboratory of Polymer and Colors Chemistry and Technology, Department of Chemistry, Aristotle University of Thessaloniki, 54124, Thessaloniki, Greece
[c] Laboratory of Advanced Materials and Devices, Department of Physics, Aristotle University of Thessaloniki, 54124, Thessaloniki, Greece
[d] AXIA Innovation GmbH, Fritz-Hommel-Weg 4, 80805, München, Germany

A B S T R A C T

The present research work focuses on the modification of Kraft lignin with phosphorus and nitrogen functionalities, and their subsequent evaluation as flame retardant additives in HDPE composites. Lignin is an inexpensive bio-based compound; this study focuses on modified lignins as environmentally friendly alternatives to the current state of art flame retardant additives, that include highly halogenated and mostly toxic compounds. Modified lignins were incorporated to HDPE in loadings ranging from 1 % wt. to 30 % wt. and the resulting composites were further studied. The produced HDPE/modified lignin composites were found to have a higher char residue and a higher temperature of maximum weight loss compared to HDPE/pristine Kraft lignin composites. Furthermore, up to 5 % modified lignin loading, the composites maintained or slightly improved the mechanical properties. Antioxidant properties were enhanced proportionally to the additive loading, with Kraft and P additives displaying the strongest antioxidant activity. Contact angle measurements of the composites on the other hand revealed a hydrophobic surface in most cases. Finally, UL-94 flame retardancy test showed lower dripping and longer burning times for all composites in comparison to neat HDPE. All these confirm the potential of lignin and modified lignins as sustainable additives for polymeric matrices.

1. Introduction

The global market of polyolefins is evaluated to reach approximately 240 billion EUR in 2025 and is expected to grow reaching 300 billion EUR by 2030 reflecting a CAGR of 4.88 % over the forecast period [1]. The market is mainly shared between polyethylene (PE) and polypropylene (PP) that account for the vast majority of polyolefins, with PE typically holding a slightly larger share due to its widespread use in packaging, films, and containers. More specifically, based on the Global Growth Insights market report, HDPE market is valued at approximately 80 billion EUR in 2025 and is expected to grow to approximately 115 billion EUR by 2033, with a CAGR of 4.35 % [2]. On the other hand, in the last two decades, environmental concerns including climate change and environmental pollution caused by non-degradable, primarily fossil-based materials, coupled with depleting oil reserves and steadily rising oil prices, have forced scientists worldwide to seek greener alternatives with an ever-increasing focus on biodegradable, bio-based and recyclable materials. This market context underscores the relevance of exploring new HDPE composites, especially since industries seek sustainable high-performance alternatives to conventional polymers. One could argue that partially replacing synthetic polyolefins by bio-based fillers is a beneficial approach in order to reduce the impact of human activities on the environment and the reliance on fossil resources [3]. When the filler endows the polyolefin with additional properties, novel materials with added value are obtained. The incorporation of bio-based fillers is also an interesting strategy in the upcycling of polyolefins [4]. Given the widespread availability and low cost of lignins, innovative bio-composites derived from industrial lignins can serve as sustainable alternatives to conventional plastic materials produced from petroleum-based resources [3,5].

* Corresponding author.
** Corresponding author.
E-mail addresses: a.tiniakos@creativenano.gr (A.F. Tiniakos), christinasamiotaki@gmail.com (C. Samiotaki), azampouli@chem.auth.gr (A. Zamboulis), a.grigoropoulos@creativenano.gr (A. Grigoropoulos), s.koutsourea@creativenano.gr (S. Koutsourea), etarani@physics.auth.gr (E. Tarani), ateknetz@physics.auth.gr (A. Teknetzi), gvourlia@auth.gr (G. Vourlias), a.karathanasis@creativenano.gr (A. Zoikis Karathanasis), dbic@chem.auth.gr (D.N. Bikiaris), ide@axia-innovation.com (I. Deligkiozi).

https://doi.org/10.1016/j.polymer.2025.129495
Received 10 August 2025; Received in revised form 2 December 2025; Accepted 16 December 2025
Available online 19 December 2025

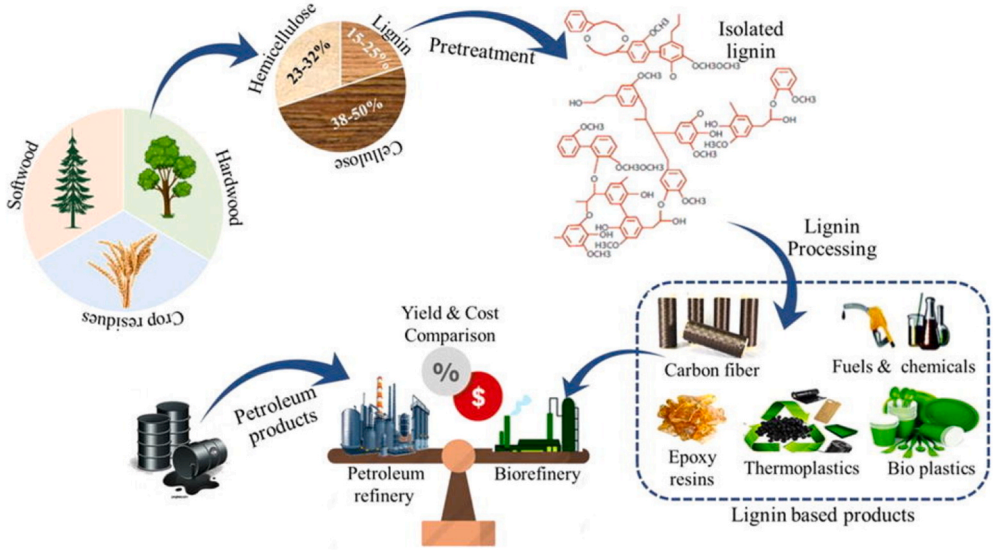

Fig. 1. The cycle of lignin isolation, processing and valorisation and the potential benchmarks to fossil refinery products [8].

Cellulose is the most abundant polymer on earth with a whopping annual production of 1.5 trillion tons, primarily used to produce paper, cardboard etc. in the pulping industry. Lignin, a by-product of the pulping industry, is the second largest naturally occurring carbon source, with a global market size of 1.3 billion EUR in 2024, that is expected to steadily increase reaching 1.7 billion by 2030, growing at a CAGR of 4.4 % from 2025 to 2030 [6], Fig. 1. Lignin is made up from three phenylpropane-derived lignol monomers: coniferyl alcohol, sinapyl alcohol and paracoumaryl alcohol, and heterogeneity arises from the diversity and degree of crosslinking of these lignols. One of the major challenges in exploiting lignin's full potential in the industrial production of composite materials is the structural variability of lignin raw material, which depends mainly on the plant source it was derived from and the extraction method used [7]. The two main types of lignin are sulfur-containing lignin, for example Kraft lignin, which accounts for >90 % of produced lignin, and sulfur-free lignin such as Soda and organosolv lignin.

When combined with an apolar polymeric matrix, lignin's heterogeneity and highly hydrophilic nature can potentially result in undesirable phenomena such as phase separation and aggregate formation. Owing to the incompatibility and poor affinity between the matrix and the additive, poor mechanical properties can be observed [3,9,10]. Lignin chemical modification is one of the most common solutions usually applied to improve the compatibility of lignin with polymeric matrices. This procedure typically includes three primary directions: (1) lignin fragmentation or depolymerization leading to chemicals rich in aromatic structures, (2) introduction of new functional groups that may then be further modified, and (3) hydroxyl group functionalization through their reaction with various agents [10,11].

Development of chemical modifications of lignin such as esterification, acetylation, phenolation, oxidation, amination, and polymer grafting has been extensively reported [12]. Esterification is among the most common methods applied for lignin chemical modification and results in improved resistance to microbial decay, enhanced UV absorption and altered thermal and mechanical properties [13–15]. Amination of lignin *via* Mannich reaction is also a quite established method of modification which provides improved properties. Specifically, enhanced thermal stability and char formation [16,17], as well as improved elasticity [18] and anti-aging performance [10,19], have been reported for various composite materials with aminated lignin. Lee et al. studied the effect of phosphorylated lignin incorporated in PP [20]. The composites presented enhanced thermal stability (increased onset of thermal degradation and increased residual mass), albeit at the expense of the mechanical properties, that deteriorated with the increase of the filler concentration.

Simultaneous phosphorous and nitrogen chemical modification has also been investigated. In PLA [21] and PP [22,23] composites, phosphorus-nitrogen modified lignins proved to be highly effective in increasing thermal stability and decreasing flammability. Yan et al. used phosphorous-nitrogen modified lignin in combination with ammonium polyphosphate and ethylene-octene copolymer to increase flame retardancy in HDPE composites [24]. Indeed, using a combination of ammonium polyphosphate/phosphorous-nitrogen modified lignin (3:1 mass ratio) increased significantly the flame retardancy of the composite. Nevertheless, HDPE's high hydrophobicity has hampered the incorporation of bio-based additives, which are typically hydrophilic, despite its promising potential.

Accordingly, we were interested in incorporating lignin modified with phosphorus (Lig-P), nitrogen (Lig-N) or phosphorus and nitrogen (Lig-PN) to HDPE to study the impact of the filler on the thermal and mechanical behaviour of HDPE as well as any potential flame retardant effect. A series of reactions were exploited for the modification of non-wood Kraft lignin. The successful modification of Kraft lignin was confirmed by Fourier transform infrared spectroscopy (FTIR) and X-ray photoelectron spectroscopy (XPS). Composites were further obtained by melt-mixing, with a lignin and modified lignin content ranging from 1 % to 30 % by weight. Structural characterization was performed by FTIR, thermal behaviour was studied by differential scanning calorimetry (DSC) and thermogravimetric analysis (TGA), and mechanical performance was obtained through tensile testing. Additionally, water contact angle (CA) and antioxidant behaviour, as well as oxygen induction time (OIT) and flame retardancy were studied.

To the best of our knowledge, this is the first systematic investigation reporting HDPE composites incorporating nitrogen-, phosphorus-, and phosphorous-nitrogen modified lignins across a broad composition range, offering new insights into how heteroatom-functionalized lignin can enhance polymer performance, notably in terms of antioxidant properties, flame retardancy and thermal stability.

2. Materials and methods

2.1. Materials

Kraft lignin (BioPiva 100, MW 5000 g/mol)) was supplied by UPM (Finland), sodium hydroxide (pellets) from Labkem (Spain), hydrochloric acid solution, formaldehyde, N,N-dimethylformamide (DMF)

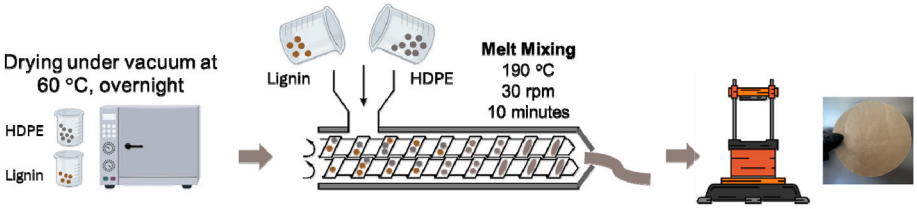

Fig. 2. Schematic presentation of the composite fabrication.

and triethylamine were purchased from Penta (Singapore). Phosphorus pentoxide (P_2O_5) was bought from Sigma Aldrich and stored in a desiccator; tetrahydrofuran (THF) was acquired from CarloEbra (Italy). Imidazole, polyethyleneimine (PEI) and phosphoryl trichloride ($POCl_3$) were supplied from Thermo Fisher Scientific, and methanol from AppliChem Pancreac. High-density polyethylene (HDPE LITEN MB 71 (MFR (190/2.16): 8 g/10 min)) was kindly provided by SILON s.r.o. (Czech Republic). In-house reverse osmosis (RO) water was used for all lignin modification reactions.

2.2. Methods

2.2.1. Synthesis of modified lignins

2.2.1.1. Synthesis of aminated lignin (Lig-N). Polyethyleneimine branched MW = 10,000 (PEI) (4.80 g, 0.48 mmol) was dissolved in H_2O (50 mL) under stirring. A 2-neck 1L round bottom flask equipped with a magnetic stirring bar under stirring was successively charged with H_2O (300 mL), 20 % w/v $NaOH_{(aq)}$ (0.5 mL), the PEI solution (4.80 g in 50 mL) and Kraft lignin (20.00 g). Formaldehyde (4.8 g, 14 mL) was then added, followed by H_2O (100 mL) and the mixture was left to stir for 5 h at 50 °C while controlling the pH between 10 and 11 by the addition of 20 % w/v $NaOH_{(aq)}$ as required at regular intervals. Then the mixture was heated to 70 °C for 1 h before cooling to room temperature. The product was precipitated by the dropwise addition of 10 % v/v $HCl_{(aq)}$ until pH 3. The dark brown precipitate was collected via vacuum filtration and washed thoroughly with H_2O until rinsings were pH $\geq$ 6. The filter cake was then dried in a vacuum oven at 40 °C overnight to furnish Lig-N (20.00 g).

2.2.1.2. Synthesis of phosphorylated lignin (Lig-P). Phosphorylated lignin was synthesized using a procedure adapted from the literature [25]. To a 500 mL round bottom flask equipped with a magnetic stirrer bar and a reflux condenser, under nitrogen, was added P_2O_5 (40.00 g, 140.8 mmol) and THF (220 mL), followed by Kraft lignin (20.00 g). The stirred suspension was then heated to reflux for 7 h before cooling to room temperature. At this point a viscous heterogenous mixture was obtained that was diluted with H_2O (200 mL) to ensure any unreacted P_2O_5 was hydrolysed to phosphoric acid. The product was isolated using vacuum filtration and washed thoroughly with H_2O until filtrate had pH $\geq$ 6. Finally, the product was dried in a vacuum oven at 40 °C overnight to furnish Lig-P (24.00 g).

2.2.1.3. Synthesis of PN functionalized lignin (Lig-PN). Lig-PN was prepared similarly as described in literature for hydroxymethylated lignin starting material [23]. Firstly, to prepare the intermediate phosphoroaminochloride, imidazole (3.40 g, 50 mmol), triethylamine (20 mL, 144 mmol) and phosphoryl trichloride (4.70 mL, 50 mmol) were dissolved in DMF (20 mL) in a 250 mL 2-neck round bottom flask purged with nitrogen, equipped with a magnetic stirrer bar and a reflux condenser. The bright orange mixture was heated to 80 °C under vigorous stirring and a nitrogen atmosphere for 8 h. After this time a viscous black slurry was obtained to which was added dropwise a pre-prepared mixture of Kraft lignin (5.00 g) and triethylamine (10 mL, 72 mmol) in DMF (30 mL). Then the mixture was heated to 95 °C and stirred for a further 12 h before cooling to room temperature. Methanol (100 mL) was added to quench any unreacted phosphoryl trichloride and to dilute the mixture and stirring continued for another 2 h. The precipitate was collected using vacuum filtration and washed thoroughly with H_2O (5 L) to remove any salts and excess DMF. Finally, the product was dried in a vacuum oven at 40 °C overnight to isolate Lig-PN (7.10 g).

2.2.2. Preparation of HDPE-lignin composites

For the preparation of the composites (Fig. 2), HDPE, Kraft and the modified lignins were dried under vacuum at 60 °C, overnight. A Haake-Buchler reomixer (model 600, Haake-Buchler Instruments Ltd., SaddleBrooke, NJ, USA) with roller blades and a mixing head with a volumetric capacity of 10 cm^3 was used for the melt-mixing. The experiments were carried out for 10 min, at 190 °C and 30 rpm, and the final samples contained lignin at concentrations 1, 5, 10, 20, and 30 wt %. An Otto Weber Type PW 30 hydraulic press coupled with an Omron E5AX Temperature Controller (Grunbach, Germany) was used to shape the melt-mixed materials into films at a temperature of 190 ± 5 °C.

2.2.3. Characterisation of modified lignins

Dynamic light scattering (DLS) was used to evaluate the particle size of Kraft lignin and modified lignins using the Litesizer 500 particle Analyzer (Anton Paar, Graz, Austria). Prior to analysis a dispersion in water was prepared at approximately 70–200 ppm depending on and adjusted accordingly to achieve 25–35 % transmittance. All measurements were performed no less than three times. Fourier transform infrared (FTIR) spectra were recorded on a Tensor 27 spectrometer, Bruker instrument fitted with a diamond ATR accessory at a specific resolution of 4 cm^{-1} in the wavenumber range from 600 to 4000 cm^{-1} in transmittance mode. The baseline of all presented spectra was corrected, and spectra was normalized.

^{31}P nuclear magnetic resonance spectrum was recorded on an Agilent AM 600 operating at a frequency of 600 MHz for protons. Lig-P was dissolved in DMSO-d_6 and 64 scans were recorded (relaxation delay 1s).

X-ray Photoelectron Spectroscopy (XPS) measurements were conducted using a Kratos Analytical AXIS Ultra^{DLD} system, featuring an aluminum monochromatic X-ray source (λ_{Ka} = 1486.6 eV) and under ultra-high vacuum conditions (10^{-9} Torr). Survey spectra (0–1200 eV) were collected with an analyzer pass energy of 160 eV and 105 W applied to the X-ray gun. High-Resolution (HR) spectra were acquired with a pass energy of 20 eV set for the analyzer and 150 W applied to the X-ray gun, during a three-sweep scan. XPS spectra were calibrated with reference to the C 1s peak at 284.6 ± 0.2 eV from C–C bonds to correct for any surface charging effect. The background of HR spectra was subtracted using Shirley or linear baselines, and the experimental curves were fitted using a combination of Gaussian (70 %) and Lorentzian (30 %) distributions. For quantitative analysis, the relative sensitivity factors (RSF) of each element were obtained from the Vision 2.2.10 software database.Inductively coupled plasma (ICP) measurements were performed on an MPAES Agilent 4210 instrument.

Thermogravimetric analysis (TGA) was conducted using a Q50 TGA model from TA Instruments (New Castle, DE, USA). The samples were placed in a platinum pan and heated within the temperature range from room temperature up to 750 °C at a heating rate of 10 °C/min under air

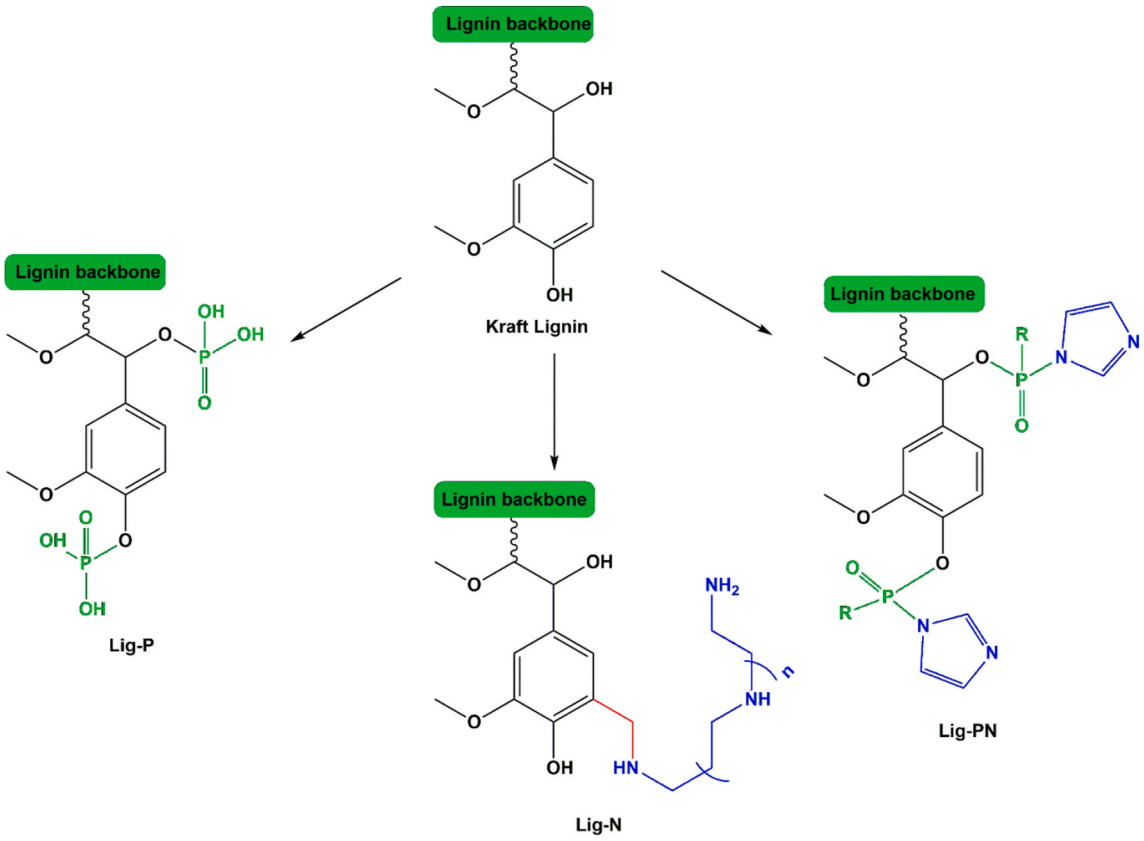

Fig. 3. Synthesis of modified lignins starting from non-wood Kraft lignin. R represents the lignin backbone, i.e., the phosphoester tethered with lignin.

flow.

2.2.4. Characterisation of the composite materials

The FTIR spectra of the prepared materials were recorded on an FTIR-2000 instrument (PerkinElmer, Waltham, MA, USA). A thin film from each composite was prepared using a hydraulic press and placed directly on the sampler. Infrared absorbance spectra were obtained from 4000 to 450 cm^{-1} using 16 co-added scans and a resolution of 4 cm^{-1}. The presented spectra were further baseline-corrected and normalized. Differential scanning calorimetry (DSC) analysis was performed using A PerkinElmer Pyris DSC-6 differential scanning calorimeter calibrated with pure indium and zinc standards for accuracy. Samples of 5 ± 0.1 mg sealed in aluminium pans were used and all experiments were performed under N_2 atmosphere with a gas flow of 20 mL/min. The samples were heated from 25 °C to 200 °C (at a rate of 10 °C per minute) to erase any thermal history, cooled to 25 °C and reheated to 200 °C with the same rate. The *Tm* and ΔH_m data were obtained from the second heating run. Oxidation induction time (OIT) was calculated after heating the composites under O_2 flow (20 mL/min) with a rate of 20 °C/min (PerkinElmer Pyris DSC-6 instrument). About 5–10 mg of each composite was placed in an aluminum pan and heated from 30 °C to 200 °C (rate: 20 °C/min) under nitrogen flow. After 3 min of isothermal heating, the gas flow was changed to O_2 and the heat flow was recorded until an exothermic peak appeared. The OIT value is defined as the time between the switching of the gas to O_2 and the appearance of the exothermic signal. The thermogravimetric analysis (TGA) of the composites was conducted using a SETARAM SETSYS TG-DTA 16/18 apparatus. 3 ± 0.5 mg samples were placed in alumina crucibles, while an empty crucible served as a reference. The experimental curve was removed after a blank measurement was made to eliminate the buoyancy effect. The HDPE/lignin composites were subjected to heating from ambient temperature to 600 °C, at a rate of 20 °C/min, under a nitrogen flow of 50 mL/min. Throughout this study, heat flow, sample mass, temperature, and their first derivatives were continuously recorded.A MiniFlex II X-ray diffraction (XRD) system (Rigaku, Co., Tokyo, Japan) was utilized to record the XRD diffractograms of the prepared composites with Cu Kα radiation (0.154 nm). The diffractograms were obtained from 5° to 45° (2θ) at a scanning rate of 1°/min. Compression molding was performed to prepare composite films for the analysis at 190 °C. After that, the films were cooled at room temperature. Tensile tests were performed using a Shimadzu EZ Test Tensile Tester, Model EZ-LX, with a 2 kN load cell, according to ASTM D882 [26], using a crosshead speed of 5 mm/min. Dumb-bell-shaped specimens were prepared using a Wallace cutting press (central portions 5 × 0.5 mm thick, 22 mm gauge length). A minimum of five measurements were performed for each composite, and the results were averaged to obtain the mean values of Young's modulus, stress at break and elongation at break.Water contact angle (CA) measurements were performed using an optical tensiometer, One Attention (Biolin Scientific, Espoo, Finland). The sessile water droplet method was used to investigate the hydrophilicity of the HDPE/lignin composite films used at different loadings. Measurements were performed in quadruple and the mean value is reported.To ensure the required conductivity of HDPE/lignin composites necessary for scanning electron microscopy (SEM) high quality imaging, all composites were gold coated using a SC7620 'Mini' Sputter Coater/Glow Discharge System (Quorum Technologies LTD, UK). SEM images were recorded on a TESCAN VEGA COMPACT instrument which provided detailed surface images essential to understand the distribution of components and interactions within the HDPE/Lig composites. Samples were mounted onto the sample holder using double-sided carbon tape. For transmission electron microscopy (TEM) imaging a latest generation Field Emission Gun Transmission Electron Microscope (Talos F200X) was utilized.The antioxidant activity of the HDPE composites was evaluated by monitoring the reduction of the 2,2-diphenyl-1-picrylhydrazyl (DPPH) radical in the composite's presence, *via* UV–Vis spectroscopy. This technique measures the ability of a substance to scavenge free radicals

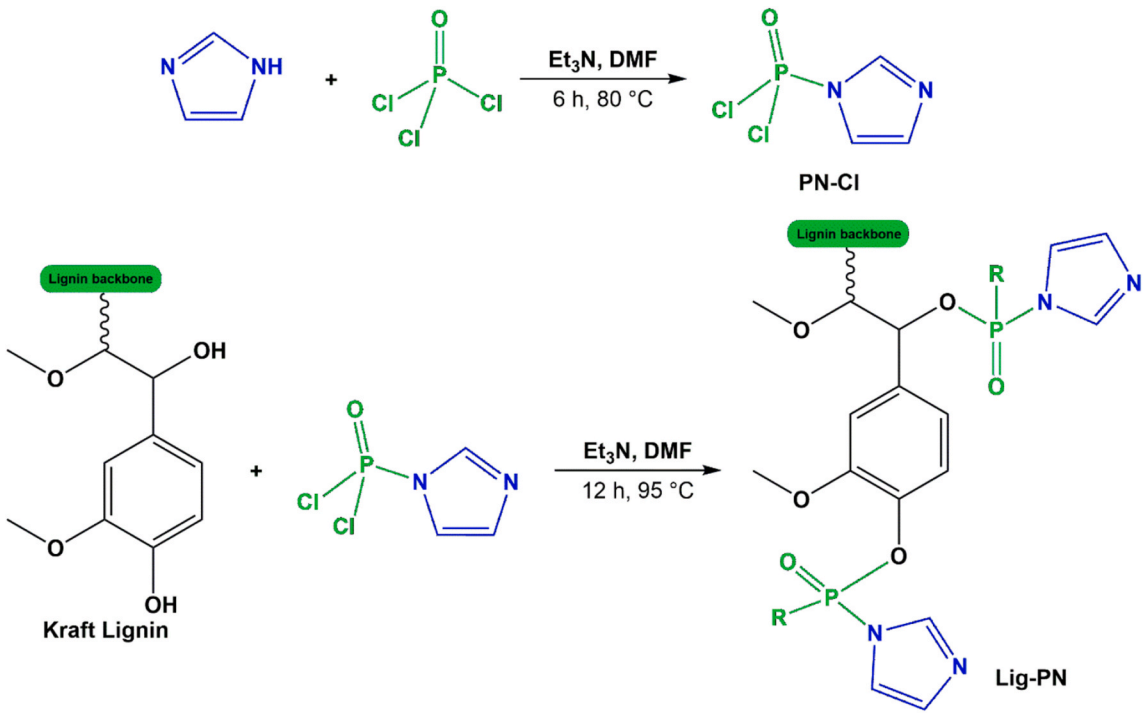

Fig. 4. Synthesis of Lig-PN starting from Kraft lignin.

by observing the decrease in absorbance of a DPPH solution after incubation with the test sample. A 0.079 mM DPPH solution in EtOH was prepared and stored in the dark for 16 h at room temperature. Films of the composites (1 cm × 1 cm) were immersed in 3 mL of the DPPH/EtOH solution at room temperature and kept in the dark. The composites' antioxidant capacity was determined by measuring the absorption decay at 517 nm at regular time intervals via UV–Vis. The residual DPPH content in the solution was calculated using Equation (1):

$$\textit{Residual DPPH content}\ (\%) = 100 - 100^{*}\frac{A_0 - A_1}{A_0} \quad (1)$$

where A_0 is the absorbance of the control sample and A_1 is the absorbance in the presence of the films. An Agilent Cary 60 UV–Vis instrument runed in absorbance mode was used to record UV–Vis spectra.

Flame retardancy was measured according to UL94 standard. A 100 mm specimen was fixed on a vertical axis. The flame was angled at 45° ± 1° to the vertical axis and the was brought at 20 mm of the bottom of the specimen (top of blue colour). The flame was applied for 30 s and then removed. When the specimen did not burn, the flame was applied for a second 30 s cycle.

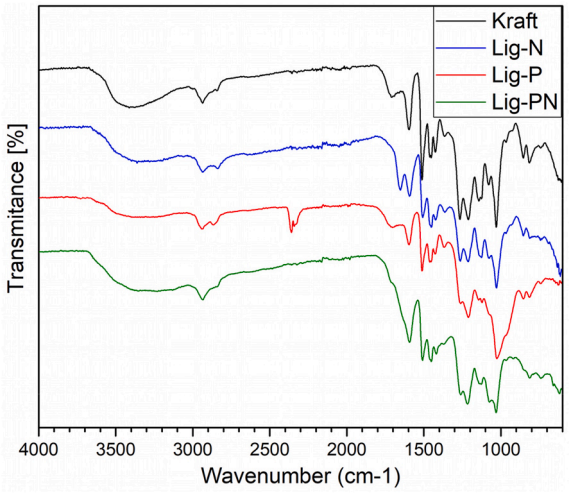

Fig. 5. FTIR-ATR spectra of Kraft and modified lignins in transmittance mode.

3. Results and discussion

3.1. Kraft lignin modification

In the present work, three different modifications of lignin (non-wood Kraft lignin) were studied (Fig. 3) and their impact on the properties of HDPE composites was further investigated. The work was motivated by the necessity for more environmentally friendly flame retardants, and thus functionalities well-known for their flame-retardant effect were incorporated into lignin: nitrogen (Lig-N) and phosphorous (Lig-P). Moreover, a lignin containing both of phosphorous and nitrogen (Lig-PN) was also prepared.

In more detail, the incorporation of amine functional groups to the backbone of lignin was accomplished by a Mannich reaction using PEI and formaldehyde under basic conditions, thus yielding Lig-N. The phosphorylation of lignin was achieved using P_2O_5 in THF at reflux, following a procedure reported by Prieur et al. [25]. Finally, a two-step one-pot reaction was applied for the synthesis of Lig-PN, Fig. 4. A phosphoroaminochloride intermediate was prepared *in situ* from phosphoryl trichloride and imidazole, and Kraft lignin was further added. The electrophilic phosphorous atom of the phosphoroaminochloride intermediate was then attacked by the deprotonated hydroxyl groups of lignin (deprotonation by triethylamine) affording Lig-PN.

Successful synthesis was confirmed by infra-red spectroscopy. Kraft lignin shows a broad stretch at 3405 cm^{-1} which is assigned to the –OH groups (Fig. 5). The strong stretching vibration at 1711 cm^{-1} is assigned to C═O groups from unconjugated ketones, carboxyl and ester groups present in the lignin backbone. Symmetric aryl ring stretch shows a sharp peak at 1595 cm^{-1} whereas asymmetric aryl ring stretch shows a strong peak at 1512 cm^{-1}. The sharp signal at 1452 cm^{-1} corresponds to the asymmetric C–H deformation from the $–OCH_3$ groups present whereas the weak signal at 1365 cm^{-1} represents the symmetric C–H

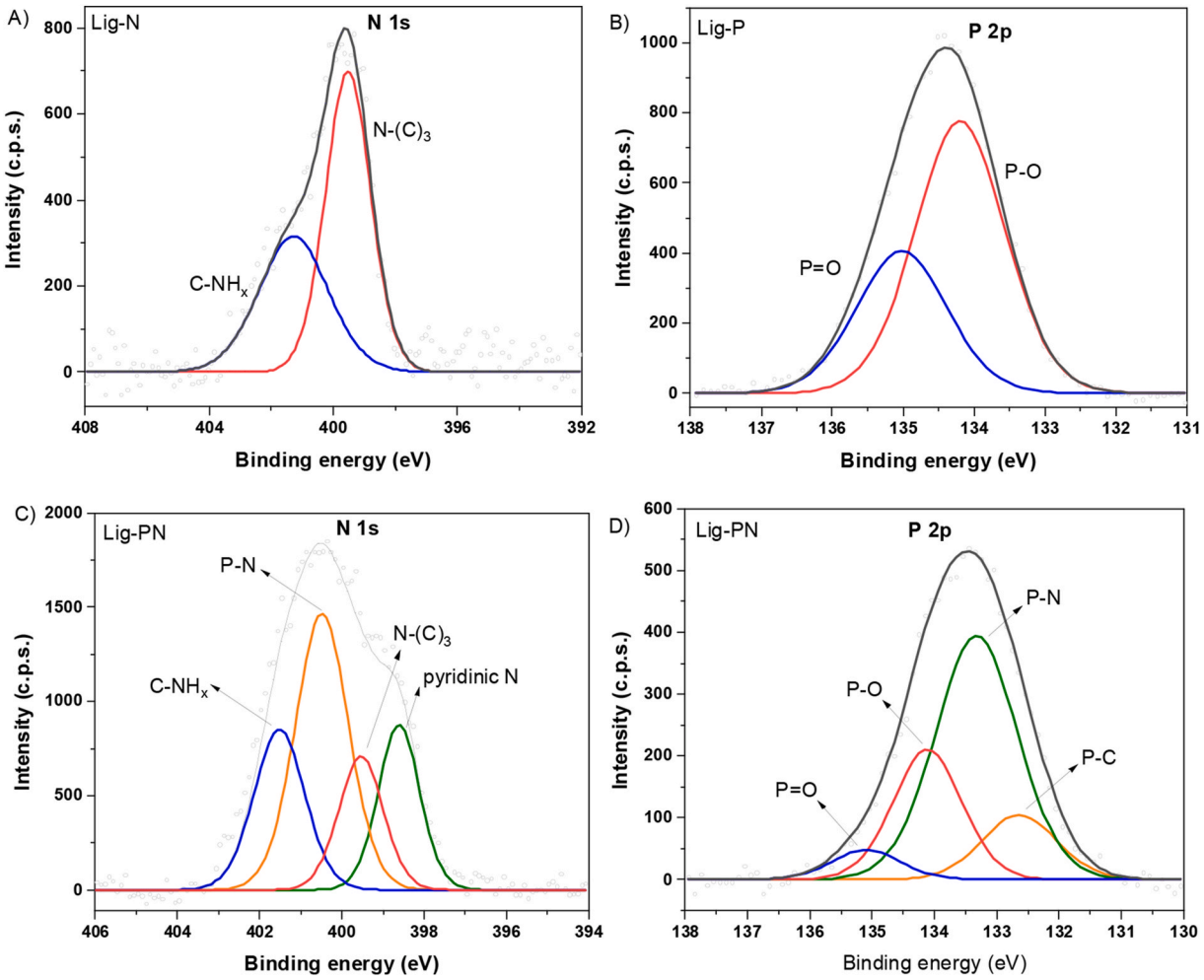

Fig. 6. A) High-resolution spectrum of N 1s core level of Lig-N. B) High-resolution spectrum of P 2p core level of Lig-P. C) and D) High-resolution spectrum of N 1s core level and P 2p core level of Lig-PN.

deformation from the –OCH_3 groups. The strong signals at 1267 cm^{-1} and 1211 cm^{-1} correspond to aryl breathing with C═O stretch and C–C, C–O and C═O stretch respectively. Aromatic C–H in plane deformation peaks are located at 1144 cm^{-1}, 1126 cm^{-1} and the strong signal at 1030 cm^{-1}. Finally, the medium shift at 1080 cm^{-1} is assigned to C–O deformation from secondary alcohols and aliphatic ether groups.

Compared to pristine Kraft lignin, the O–H and N–H stretching band at 3350 cm^{-1} changed after the modifications. More specifically for Lig-N, its intensity increased notably, which is also true for the C–H stretching vibration at 2985 cm^{-1}. A new peak corresponding to the N–H bending in Lig-N at 1653 cm^{-1} was additionally observed. The C–H aryl ring stretch at 1508 cm^{-1} decreased considerably as expected since C–H bonds are substituted by C–C bonds in the modification reaction. Finally, C–H deformation at 814 cm^{-1} was greatly reduced in Lig-N spectra.

The stretching vibration of O–H at 3405 cm^{-1} decreased in Lig-P compared to pristine lignin. On the other hand, C–H stretch of methyl and methylene groups at 2865 cm^{-1} increased in intensity whereas the symmetric aryl ring stretch at 1595 cm^{-1} decreased which was also true for the aryl ring breathing with C═O stretch at 1267 cm^{-1} and aromatic C–H in plane deformations at 1144 cm^{-1} and 1126 cm^{-1}. A significant increase in P–O stretching vibration at 1026 cm^{-1} was observed as well as P═O and/or $P(OH)_2$ stretching bands at 1210 cm^{-1} confirming that the phosphorylation took place successfully.

Finally, compared to Kraft lignin, in Lig-PN spectra the O–H stretching became broader and shifted to 3140 cm^{-1}. The peak corresponding to the symmetric aryl ring stretch in combination with the P═O stretching at 1595 cm^{-1} also broadened and intensified compared to pristine lignin. The C–H aryl ring stretch at 1508 cm^{-1}, as well as the aryl ring breathing with C═O stretch at 1267 cm^{-1} and the aromatic C–H in plane deformation at 1144 cm^{-1} and 1126 cm^{-1} decreased considerably. P═O and/or $P(OH)_2$ stretching bands were observed at 1210 cm^{-1}, whereas a new peak was observed at 1070 cm^{-1} which was attributed to the P–N–C vibration.

Due to the limited solubility of the modified lignins in $CDCl_3$/pyridine, OH quantitative characterization with ^{31}P spectroscopy could not be performed [27]. Nevertheless, ^{31}P liquid NMR spectrum in DMSO-d_6 could be recorded for Lig-P confirming the successful phosphorylation reaction (Fig. S1). The observation of three broad peaks in the −0.91 to −1.22 ppm region suggests that both aliphatic and phenolic OH groups have been phosphorylated [25]. To overcome the limitations due to poor solubility, pristine and modified lignins were also studied by XPS. All XPS surveys exhibit major peaks of carbon and oxygen, which are the primary elements in the samples (Fig. S2). Lig-P and Lig-PN demonstrate prominent peaks of phosphorus as well, while Lig-N and Lig-PN display characteristic nitrogen peaks, thus confirming the presence of N and P in the modified lignins. The elemental composition on the surface of all lignins is reported in Table S1.

To further investigate the chemical environment of phosphorus and nitrogen, high-resolution spectra of P 2p and N 1s core levels were acquired (Fig. 6). The N 1s profile of Lig-N is well-fitted with two peaks located at 399.5 eV and 401.3 eV, which can be attributed to N-$(C)_3$ bonds and C-NH_x species, respectively. Two additional components

Table 1
ICP phosphorus determination results, lignin particle size determined by dynamic light scattering and decomposition and maximum weight loss temperatures determined by TGA.

Additive	Phosphorous content	Particle size (nm)	Initial decomposition temperature (°C)	Maximum weight loss (°C)	Char residue (%)
Kraft	–	1082 ± 246	201	471	4
Lig-N	–	1015 ± 158	203	637	8
Lig-P	3.53 %	351 ± 41 3748 ± 546	186	659	15
Lig-PN	4.86 %	256 ± 36	205	535	13

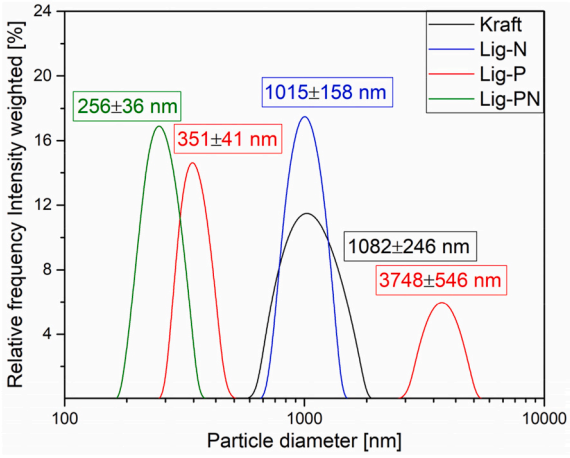

Fig. 7. Particle size distribution of modified lignins as measured by DLS. Presented in logarithmic scale.

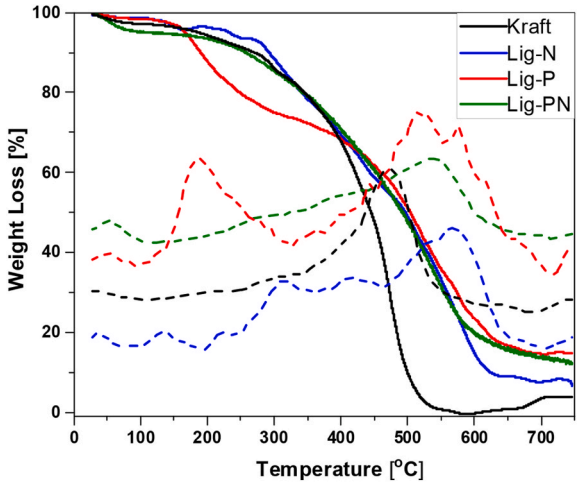

Fig. 8. TGA (continuous lines) and dTG (dotted lines) curves of modified lignins, heated at a rate of 10 °C/min under air flow.

appear in Lig-PN, with binding energy 398.6 eV and 400.5 eV. The latter corresponds to P–N bonds, which account for 41.2 % of the nitrogen bonds in Lig-PN. The value of the low-energy component is typical for pyridinic-like nitrogen. The P 2p spectrum of Lig-P is fitted with two components. The first one at 134.2 eV, which is the main contribution, originates from P–O bonds, while the second peak at 135 eV corresponds to P═O bonds. Four peaks are revealed for the P 2p spectrum of Lig-PN, with the new ones centered at 132.6 eV and 133.3 eV. The binding energy of 133.3 eV is characteristic of P–N bonds. This is the main contribution in Lig-PN, accounting for 55.9 % of the phosphorus bonds, in agreement with the analysis of the corresponding nitrogen spectrum. The peak at 132.6 eV can be related to P–C bonds. Overall, it is noteworthy that the XPS analysis confirms the successful incorporation of nitrogen and phosphorus in Kraft lignin, and the presence of P–N bonds in Lig-PN, supporting the formation of the phosphoroaminochloride adduct.

For the P-modified lignins, the successful incorporation of phosphorus was further confirmed by inductively coupled plasma (ICP), Table 1. The P content achieved was 3.5 % for Lig-P and 4.9 % for Lig-PN. The higher content observed for Lig-PN may be attributed to the higher substitution of lignin hydroxyls with the more reactive phosphoroaminochloride compared to phosphorous pentoxide.

Regarding the size of lignin particles, it is easily deduced from Fig. 7 that lignin modifications resulted in changes in particle size. For Lig-PN (particle size of 256 ± 36 nm) an obvious decrease was observed compared to Kraft lignin (1082 ± 246 nm), possibly due to electrostatic repulsion of newly formed phosphoesters. Lig-N had a narrower particle size distribution (1015 ± 158 nm) compared to Kraft lignin but similar particle size, long alkyl chains from PEI may get entangled thus preventing particle size reduction. Finally, Lig-P showed two major populations at 351 ± 41 nm and at 3748 ± 546 nm, the larger particle size population may result from the aggregation of the smaller one.

From Fig. 8 illustrating the TGA graphs of modified lignins, ignoring the initial mass loss close to 100 °C which is due to humidity present in the samples, it can be deduced that Kraft lignin, Lig-N, Lig-P and Lig-PN started to decompose at 201 °C, 203 °C, 186 °C and 205 °C respectively. Whereas maximum weight loss occurred at 471 °C, 637 °C, 659 °C and 535 °C leaving 4 %, 8 %, 15 % and 13 % char residue respectively as summarized in Table 1. Interestingly Lig-P shows a reduction in initial decomposition temperature compared to kraft lignin, whereas other modified lignins follow a similar behaviour as Kraft. As discussed in section 3.2.4, the different degradation profile of Lig-P could be attributed to the dehydrating action of phosphoric groups [20]. Maximum weight loss temperature, however, significantly increased for all modified lignins compared to Kraft with the most significant increase observed for Lig-P from 471 °C to 659 °C respectively.

Overall, all characterizations confirm the successful modification of

Table 2
Formulations of HDPE/modified-lignin composites.

Sample	HDPE (%)	Lignin (%)
Kraft 1	99	1
Kraft 5	95	5
Kraft 10	90	10
Kraft 20	80	20
Kraft 30	70	30
Lig-N 1	99	1
Lig-N 5	95	5
Lig-N 10	90	10
Lig-N 20	80	20
Lig-N 30	70	30
Lig-P 1	99	1
Lig-P 5	95	5
Lig-P 10	90	10
Lig-P 20	80	20
Lig-P 30	70	30
Lig-PN 1	99	1
Lig-PN 5	95	5
Lig-PN 10	90	10
Lig-PN 20	80	20
Lig-PN 30	70	30

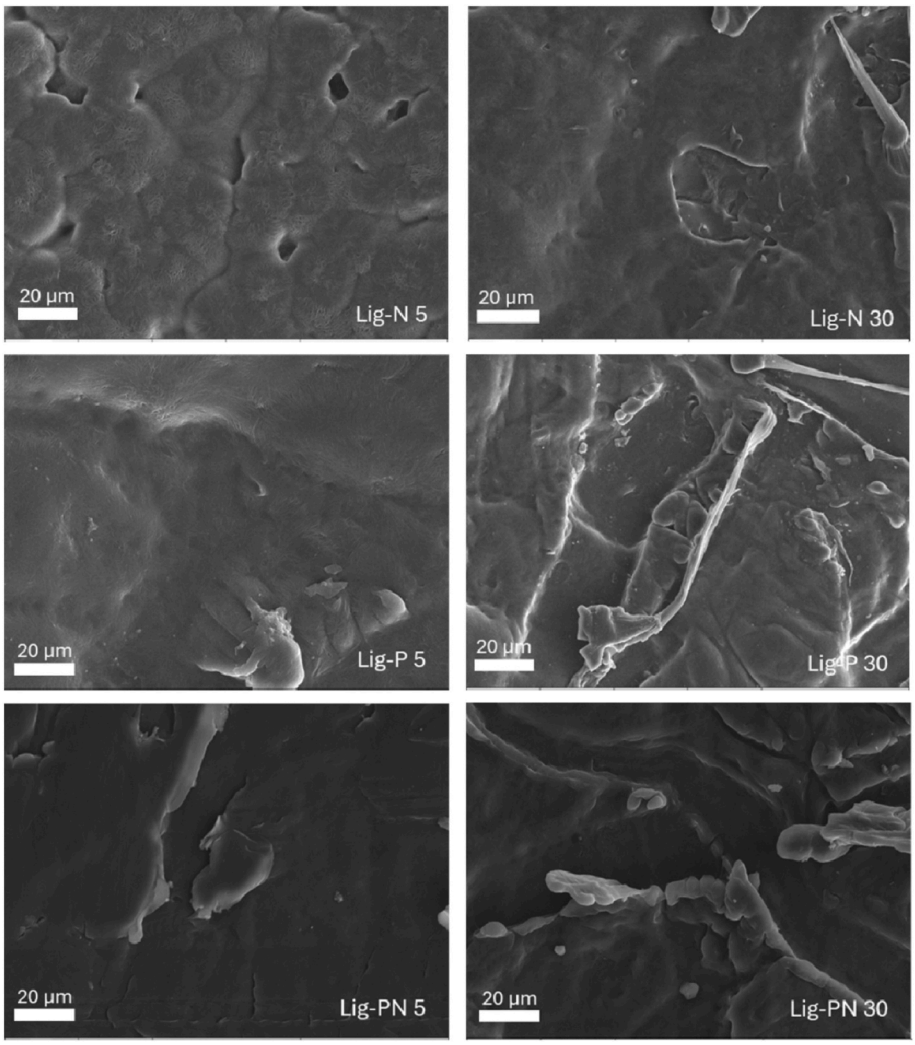

Fig. 9. SEM images of the composites with 5 % and 30 % loading of the modified lignin.

non-wood Kraft lignin and the incorporation of N- and P-containing groups. The particles size of the P- and PN-modified lignnins decreased compared to pristine lignin. Most importantly, upon modification the temperature of maximum weight loss and the char residue increased significantly, especially for the phosphorylated lignin (Lig-P).

3.2. Modified-lignin composites

3.2.1. Morphology and structural characterisation

To evaluate the potential of the P- and N- incorporation into lignin backbone and the impact of these modifications, the modified lignins were further incorporated to high-density polyethylene (HDPE) and the properties of the corresponding composites were thoroughly studied.

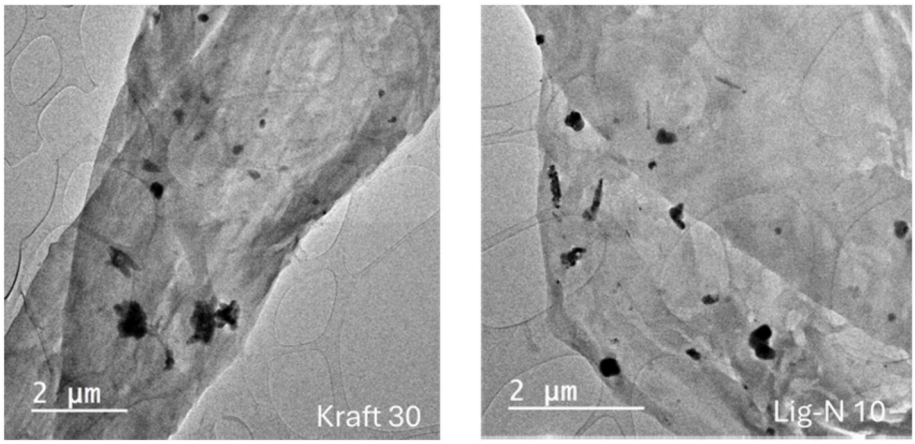

Fig. 10. TEM images of Kraft 30 and Lig-N 10 samples.

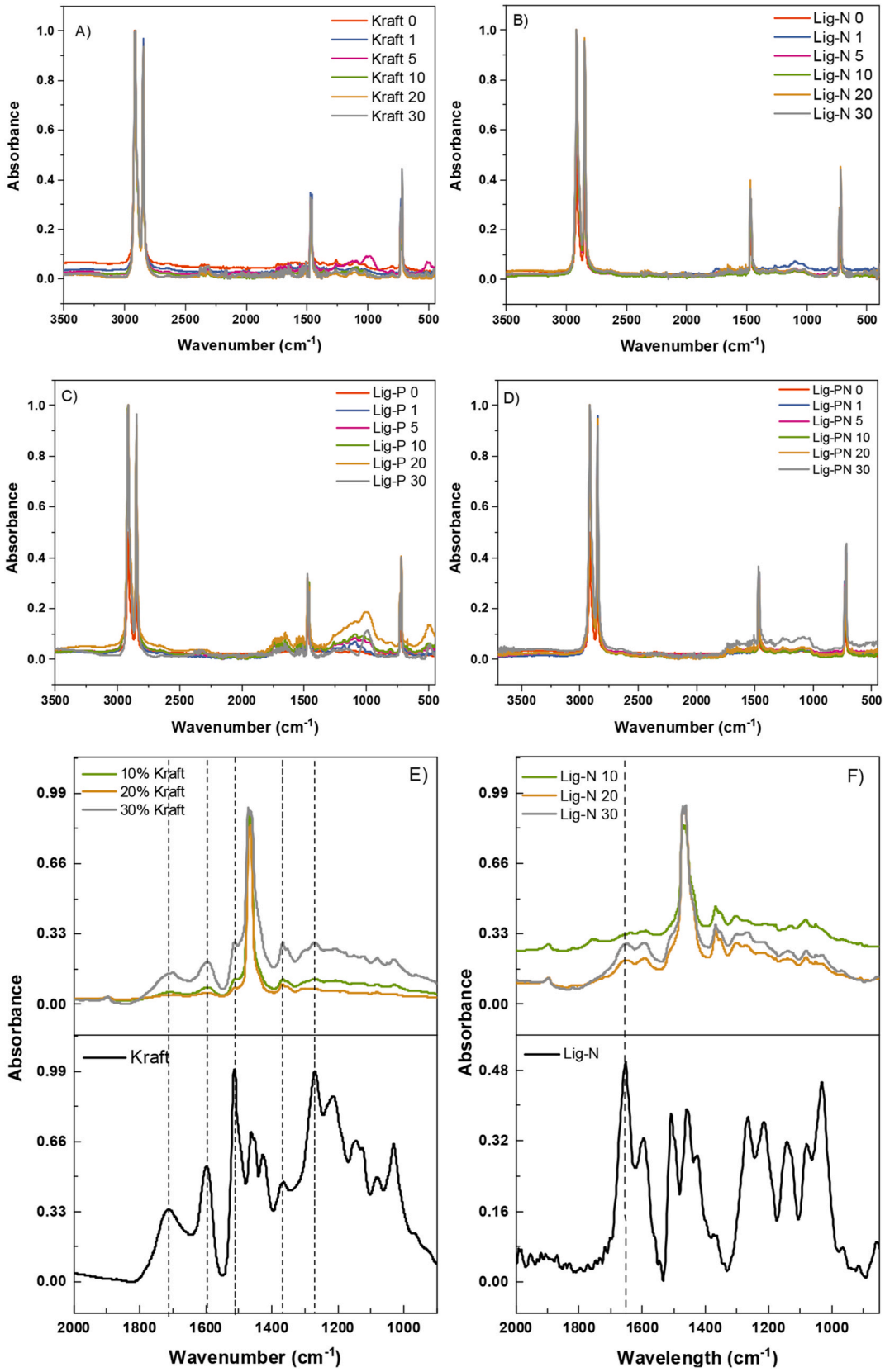

Fig. 11. FTIR spectra of the prepared Kraft, Lig-N, Lig-P and Lig-PN composites. A), B), C), D) Full spectra, E), F), G), H) zoom-in of the 850-2000 cm^{-1} region.

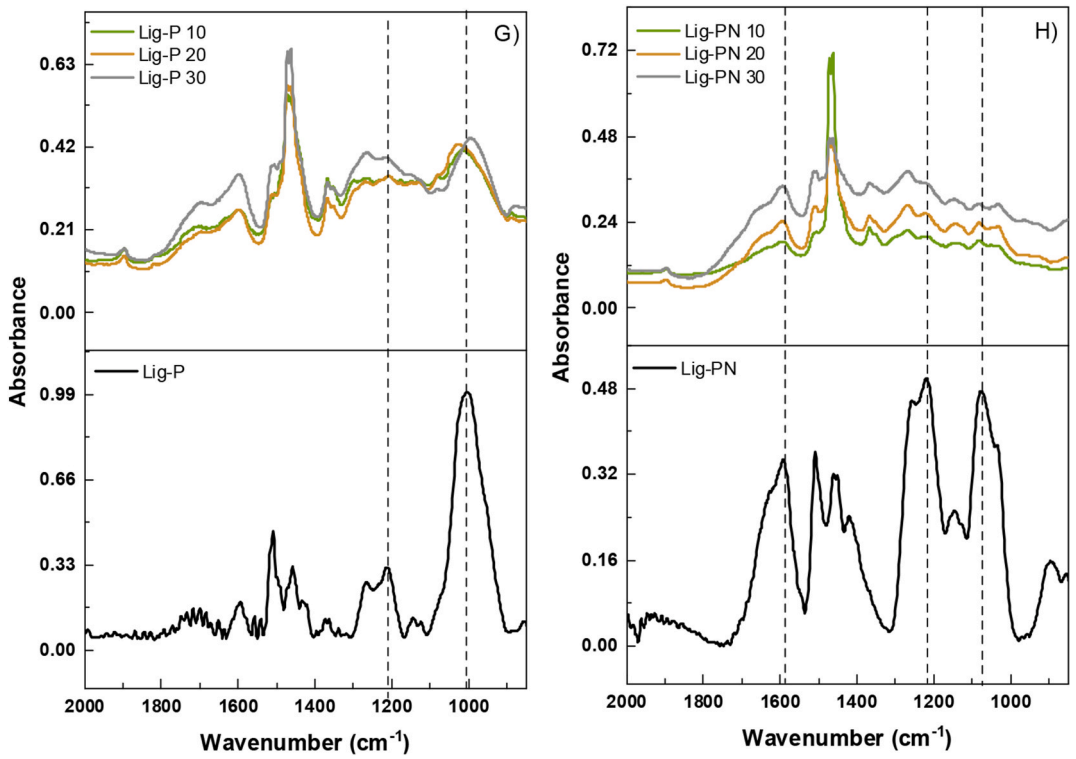

Fig. 11. (*continued*).

The composites were prepared by melt-mixing at 190 °C, at a rotational speed of 30 rpm, for 10 min. Loadings between 1 % wt. and 30 % wt. were investigated (Table 2), affording increasingly dark-coloured composites. The composites were pressed into films at a temperature of 190 ± 5 °C.

The morphology of the samples was analysed using scanning and transmission electron microscopy (SEM and TEM). Fig. 9 presents some indicative SEM images of composites containing 5 % and 30 % modified lignin. At 5 % of the filler, a smoother surface with only a small number of holes and gaps is observed. On the other hand, at additive loadings exceeding 10 % noticeably rougher surfaces and evident aggregate formation are observed, which are typical of a lower additive/matrix compatibility. This can be attributed to the relatively low affinity of the lignin additives with the hydrophobic polyethylene matrix [28]. These observations are further supported by TEM images (Fig. 10), where irregularly shaped particles are observed as well as some aggregates in both cases. Interestingly, dispersion of Lig-N within the HDPE matrix is improved compared to the Kraft material.

The FTIR spectra of the prepared composites are illustrated in Fig. 11. As anticipated, the characteristic absorbance peaks of the HDPE polymer are evident in all cases. Specifically, a double peak at 2910 cm^{-1} and 2846 cm^{-1} is associated with the symmetric and asymmetric C–H stretching vibrations, while the double peaks at 1473–1461 cm^{-1} and 730–719 cm^{-1} correspond to the bending and rocking deformation vibrations of CH_2 groups [29]. Several lignin-related peaks are also observed in the spectra of the composites, especially in samples with a lignin content exceeding 10 %.

More specifically, the characteristic absorbance bands of the composites with Kraft lignin corresponding to carbonyl (C═O) groups and aromatic ring stretching vibrations are observed at 1713, 1596, 1511, 1363 and 1269 cm^{-1}, as described earlier (Fig. 11E). The characteristic peak of Lig-N, around 1650 cm^{-1} corresponding to the N–H bending is observed in the composite materials (Fig. 11F). [22,30]. Regarding the spectra of the Lig-P composites (Fig. 11G), in addition to the three high-intensity absorbance peaks characteristic of HDPE, the distinctive vibrations of phosphorus bonds are also evident. The $P(OH)_2$ and/or

Table 3
Melting temperature (Tm), crystallization temperature (Tc), melting enthalpy (ΔHm), 5 % mass loss temperature (T_5) and temperature of maximum decomposition rate ($T_{d,\ max}$) of the prepared composites.

Sample	Tm (°C)	Tc (°C)	ΔHm (J/g)	Xc (%)	T_5 (°C)	$T_{d,\ max}$ (°C)	Char residue (%)
Neat HDPE	135	117	215	81	456	500	0.25
Kraft 1	137	113	211	73	462	510	0.71
Kraft 5	135	113	202	73	465	512	0.21
Kraft 10	134	115	166	69	448	507	4.7
Kraft 20	135	115	165	71	408	503	2.5
Kraft 30	134	115	155	70	388	501	5.4
Lig-N 1	136	117	192	66	471	511	0.1
Lig-N 5	136	117	203	73	467	511	0.1
Lig-N 10	135	116	166	69	442	504	2.3
Lig-N 20	135	116	162	63	423	498	3.7
Lig-N 30	134	117	123	60	329	502	5.5
Lig-P 1	137	115	184	63	453	510	0.2
Lig-P 5	136	115	171	61	458	508	0.7
Lig-P 10	136	117	190	72	432	511	0.7
Lig-P 20	135	117	166	71	373	510	3.8
Lig-P 30	135	117	159	70	276	506	12.5
Lig-PN 1	135	117	126	71	453	507	7.8
Lig-PN 5	138	116	139	72	455	509	4.7
Lig-PN 10	135	118	135	74	457	510	8.6
Lig-PN 20	136	118	163	72	392	509	11.1
Lig-PN 30	136	119	148	69	350	506	14.8

P═O stretching vibrations are observed at 1210 cm^{-1}, particularly in samples with lignin content exceeding 5 %. The P–O stretching vibration at 1026 cm^{-1} was also detected and displayed significantly increased intensity in samples containing 20 % and 30 % filler. Finally, concerning the HDPE/Lig-PN composites (Fig. 11H), in addition to the characteristic peaks of the neat polymer matrix, peaks at 1595 and 1210 cm^{-1} are detected, as well as an absorbance at 1080 cm^{-1} assigned to P–N–C

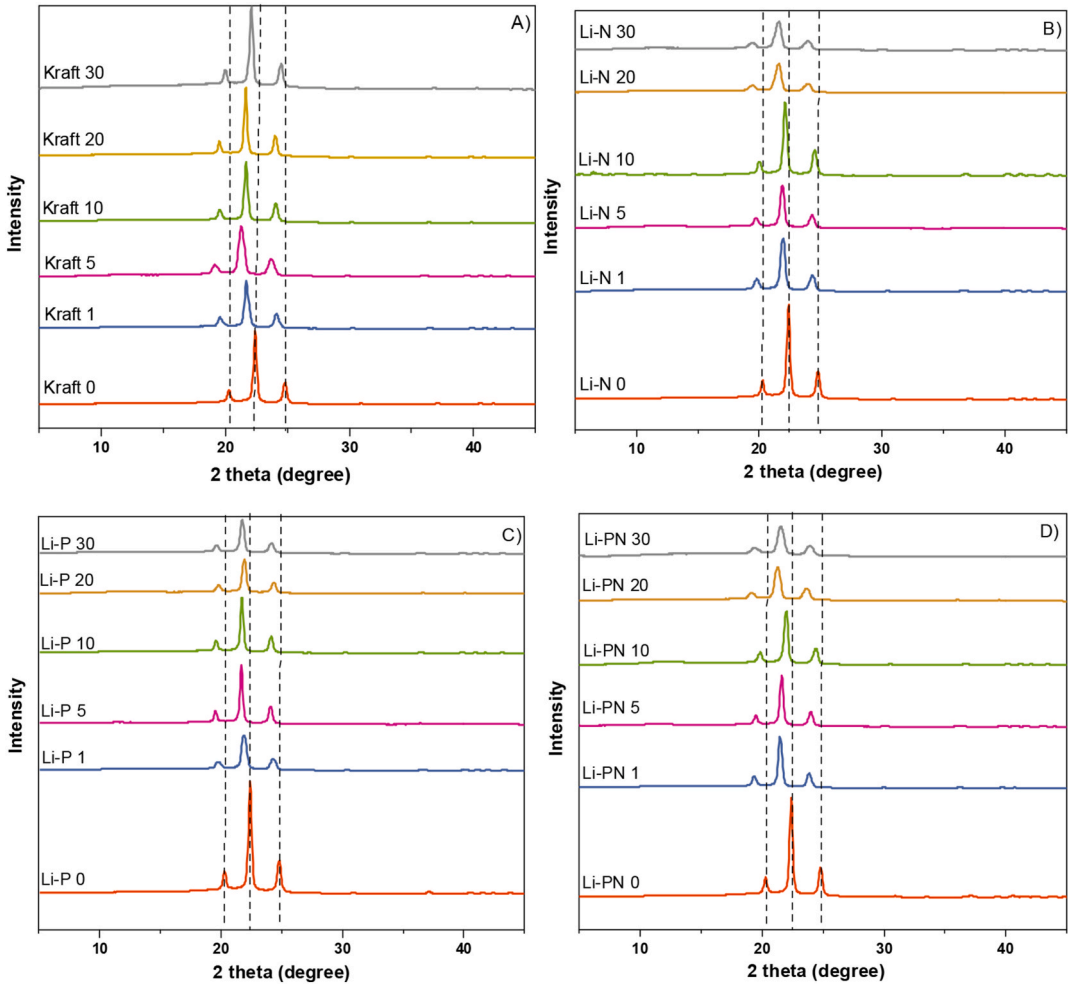

Fig. 12. XRD patterns of A) Kraft 1–30, B) Lig-N 1–30, C) Lig-P 1–30, and D) Lig-PN 1–30 composites.

vibrations. As anticipated, the intensity of these peaks increases proportionally with lignin content.

3.2.2. *Thermal transitions and crystallization*

In order to assess the melting and crystallization behaviour of the composites DSC analysis was performed. The melting point temperatures, Tm, of all composites were recorded from 134 °C to 138 °C (Table 3, Fig. S3), indicating only minor differences between the composites and between the composites and neat HDPE. This observation is in agreement with literature reports showing that lignin content up to 30 wt% leads to insignificant changes in the melting behaviour of the polymer [31], suggesting the quality of the HDPE crystals is not much affected by the presence of the additives [32]. Regarding crystallization from the melt, once more small differences are observed. It is noticeable that modified lignin composites present higher values compared to Kraft lignin composites, indicating less hindrance to HDPE crystallization [33]. The slight initial decrease in Tc suggests a weak facilitation of the crystallization process at low filler concentrations, whereas subsequent increases in lignin content may disturb crystallization [34].

This is further supported by crystallinity degree values. Crystallinity is reduced in the composites compared to HDPE, which indicates that Kraft and the modified lignins do not act as nucleating agents in this case. This may be associated with the abundance of OH groups in the lignin structure, which promote internal and external hydrogen bonding. Such bonding network may hinder the interaction of the filler with the matrix leading to diminished reinforcement efficacy [35]. Nevertheless, the crystallinity degree remains quite high in the samples containing up to 10 % of the additive despite the amorphous nature of lignin because of which we would expect a higher decrease [36]. Similar observations have been reported in the literature in other polyolefin blends with modified lignin [5,37,38], where improved compatibility between the filler and the polymeric matrix was suggested at low concentration. However, subsequent increase in the filler content up to 30 wt% resulted in a notable decrease in crystallinity indicating a possible saturation of lignin in PE matrix and consequent agglomeration of lignin particles which restrict the HDPE chain mobility during the crystallization process [38]. This observation is further supported by the reduction in the heat of fusion (ΔH_m) detected at lignin loadings higher than 10 wt%, which may be correlated with the formation of less perfect and fewer crystals [39]. Finally, the lignin particles may absorb thermal energy during heating, resulting in less energy transmission available for HDPE and delayed crystallization [40,41].

The small impact of the filler on the overall crystallinity of the samples is corroborated by XRD measurements. The XRD patterns in the 2θ range of 5°–45° for HDPE and its composites are presented in Fig. 12. For all composites, the characteristic diffraction pattern of HDPE is observed: 2θ = 24.8° and 22.4° (orthorhombic) and 2θ = 20.2° (triclinic) [34], while there are no additional peaks corresponding to the presence of lignin, since lignin is amorphous. Incorporation of the lignin-based additives results in a slight shift towards smaller 2θ angles (not more than 1.5°) and peak broadening, confirming a minor disruption of the HDPE crystalline arrangement, which increased with lignin content [34]. Finally, the reduction in the peak intensity with increasing filler content indicated a decrease in the degree of crystallinity,

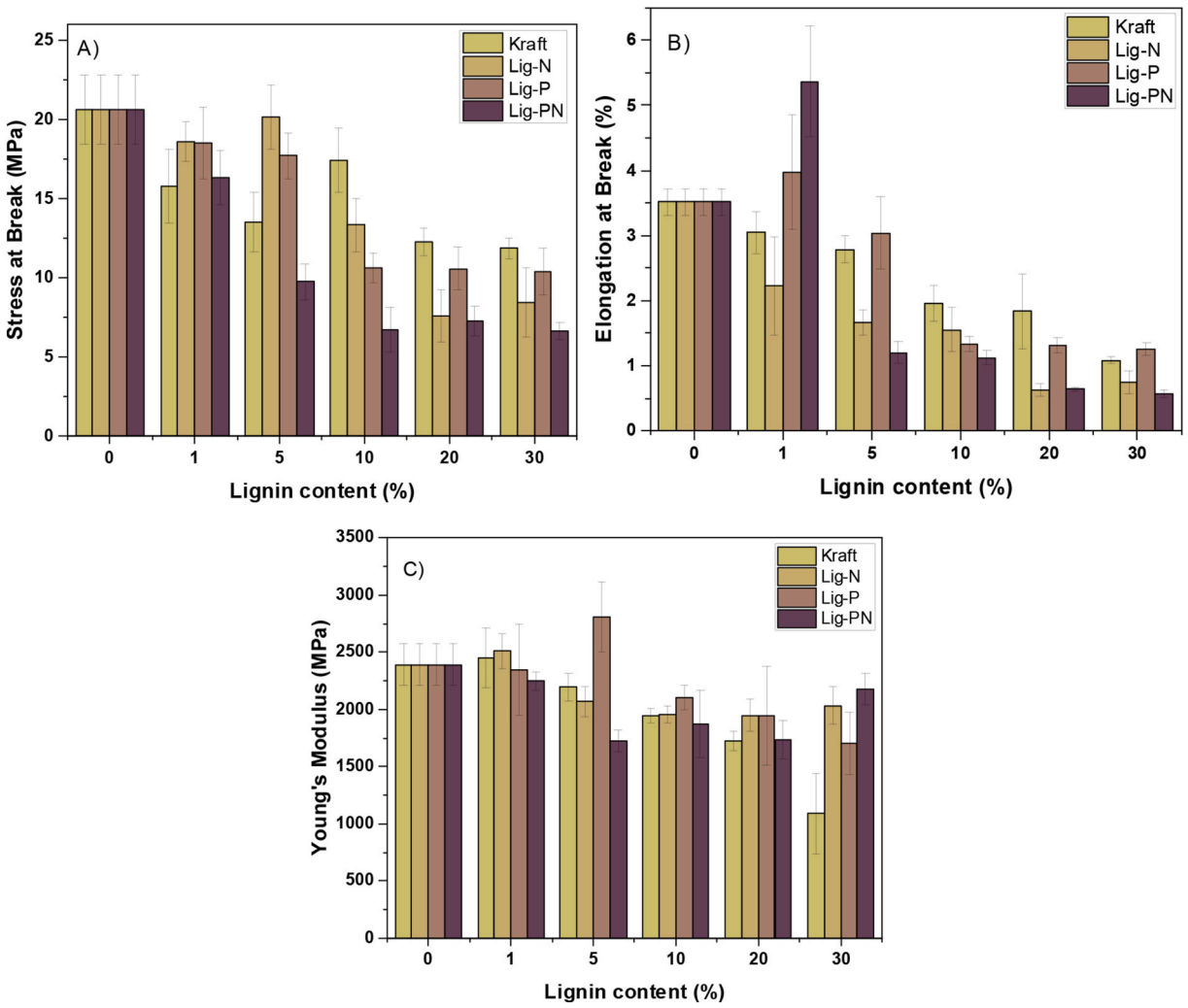

Fig. 13. a) Stress at Break, b) Elongation at Break, c) Young's modulus of HDPE-modified lignin composites from 0 to 30 % loading.

Table 4
Mechanical performances of HDPE composites.

Sample	Elongation at Break (%)	Young's Modulus (MPa)	Stress at Break (MPa)
Neat HDPE	3.5 ± 0.2	2390 ± 184	20.6 ± 1.2
Kraft 1	3.05 ± 0.2	2448 ± 262.5	15.7 ± 2.3
Kraft 5	3.1 ± 0.3	2197 ± 120.7	13.5 ± 1.8
Kraft 10	2.8 ± 0.2	1942 ± 63	17.4 ± 2.0
Kraft 20	1.9 ± 0.3	1722 ± 84	12.2 ± 0.8
Kraft 30	1.8 ± 0.6	1089 ± 355	11.8 ± 0.7
Lig-N 1	2.2 ± 0.2	2510 ± 152	18.5 ± 1.2
Lig-N 5	1.7 ± 0.8	2069 ± 131	20.1 ± 2
Lig-N 10	1.5 ± 0.2	1956 ± 78	13.3 ± 1.7
Lig-N 20	0.6 ± 0.3	1950 ± 139	7.5 ± 1.6
Lig-N 30	0.7 ± 0.1	2033.5 ± 165	8.4 ± 2.2
Lig-P 1	3.9 ± 0.2	2341.9 ± 399	18.5 ± 2.3
Lig-P 5	3.0 ± 0.9	2810.6 ± 303	17.7 ± 1.4
Lig-P 10	1.3 ± 0.5	2105.3 ± 103	10.6 ± 0.9
Lig-P 20	1.3 ± 0.1	1945.3 ± 429	10.6 ± 1.4
Lig-P 30	1.3 ± 0.2	1702 ± 274	5.2 ± 1.1
Lig-PN 1	5.4 ± 0.2	2247 ± 78	16.3 ± 1.7
Lig-PN 5	1.2 ± 0.8	1728 ± 94	9.7 ± 1.1
Lig-PN 10	1.12 ± 0.2	1871 ± 292	6.7 ± 1.4
Lig-PN 20	0.6 ± 0.1	1739 ± 170	7.2 ± 0.9
Lig-PN 30	0.6 ± 0.02	2174 ± 136	6.6 ± 0.5

consistent with the DSC findings.

3.2.3. *Mechanical behaviour*

To verify the mechanical behaviour of the composites, dumb-bell specimens were subjected to tensile testing. In general, incorporation of lignin-based additives resulted in a proportional deterioration of the overall mechanical performance. However, composites prepared with additive loadings up to 5 % of the various fillers, present satisfactory stress and elongation at break values (Fig. 13, Table 4). Specifically, Lig-N and Lig-P composites present stress at break values comparable to neat HDPE, whereas the samples with Kraft lignin demonstrated reduced properties, suggesting slightly improved interfacial adhesion with the polymer matrix [10]. In addition, Young's modulus values, particularly for the Lig-N and Lig-P composites, remain comparable to those of neat HDPE, indicating efficient load transfer in the interface between lignin particles and HDPE [42]. The stress-strain curves (Fig. S4) reveal a clear yield point followed by a plastic region before failure, suggesting moderate ductility and toughness.

On the other hand, mechanical performance deteriorated upon further increase of the lignin content (10–30 wt%). Stress at break is reduced by approximately 40 % at 20 wt% filler content indicating ineffective stress transfer to the matrix which can lead to stress concentration [43]. Elongation at break decreased significantly revealing that lignin acted as a rigid filler leading to brittle materials. This finding was further supported by the retention of Young's modulus values even at filler loadings up to 30 wt% [44]. Stress-strain curves (Fig. S4)

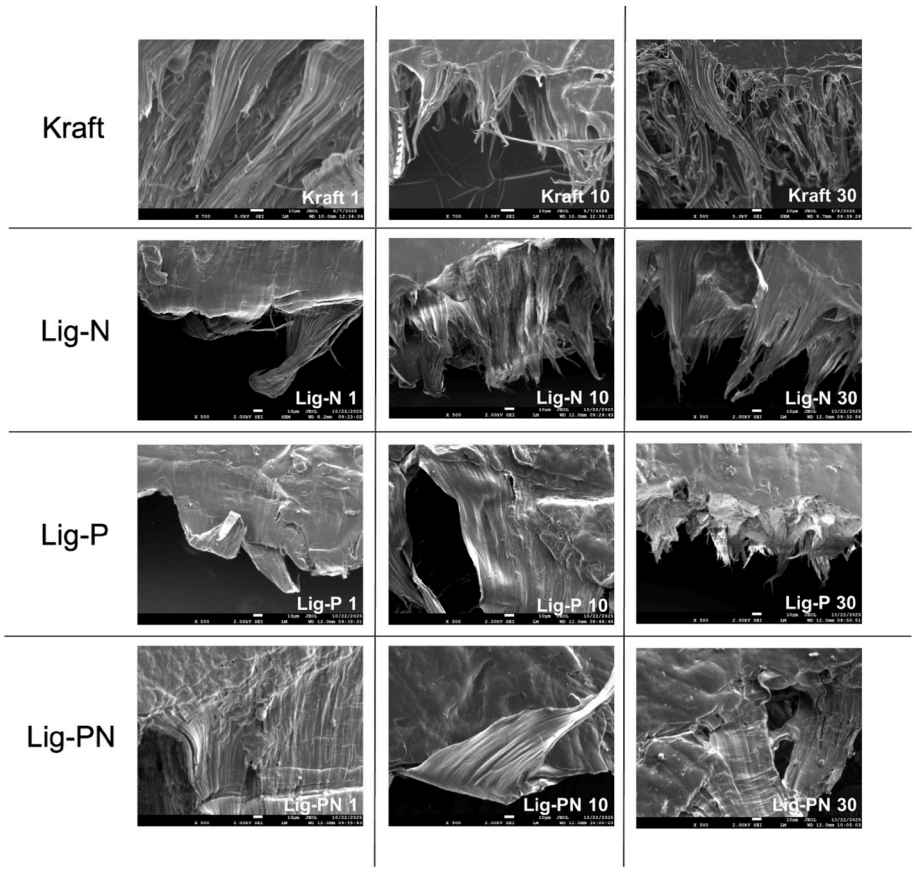

Fig. 14. SEM images of the fractured surfaces of the composites after tensile testing.

confirm these observations revealing a brittle fracture mode with a sharp stress drop immediately after the yield point, suggesting reduced toughness and limited plastic deformation. This can be correlated with the decreased crystallinity values observed from DSC measurements and poor interfacial adhesion due to polarity differences between the matrix and the filler. Moreover, it may be inferred that lignin particles act as stress-concentration sites, thereby accelerating failure and leading to earlier fracture compared to neat HDPE [45] Overall, the composites incorporating Lig-P displayed a slightly better performance.

The fractured surfaces of the HDPE/lignin composites are presented in Fig. 14. Up to 10 % of the various additives, the polymer matrix is able to withstand the lignin loading since smoother morphology is observed, particularly for Lig-N and Lig-P samples. This observation is also reflected in the lack of fiber breakage and the higher stress at break values discussed earlier. For higher lignin loadings, the SEM micrograph is typical of predominantly brittle failure. The presence of micro-voids resulted from the particle pull-out and interface friction, surrounded by abruptly cut fibrils leads to a dimpled network. Such observations indicate matrix disintegration and weak interfacial adhesion between the lignin particles and HDPE [5,46,47].

3.2.4. *Thermal and thermo-oxidative stability and flammability*

The thermal stability of HDPE/lignin composites was assessed by thermogravimetric analysis, while oxidation induction time measurements were implemented to evaluate oxidative stability. The TGA thermograms and dTG curves are presented in Fig. 15, while the temperatures corresponding to 5 % mass loss (T_5) and maximum thermal degradation rate ($T_{d,max}$) are presented in Table 3. In all examined materials, negligible mass loss was observed below 250 °C.

Regarding T_5, all composites exhibit the same trend with increasing additive content: (i) at additive loadings up 5 %, no significant change was observed, (ii) at larger loadings (10–30 % wt.), a gradual decrease was observed, suggesting a decrease of the onset of thermal degradation. The reduction in T_5 values for P-containing composites may be attributed to the catalytic effect of phosphoric acid groups, which are known to promote dehydration and accelerate initial decomposition [21]. For Kraft lignin and Lig-N a slight improvement is observed compared to neat HDPE, indicating an improvement in thermal stability at low additive content.

The $T_{d,max}$ values ranged between 500 °C and 510 °C across the various compositions, and were overall higher than for neat HDPE, suggesting an increased thermal stability at higher temperatures. Regarding Kraft and Lig-N composites, the highest $T_{d,max}$ value was observed for 5 % additive loading, after which $T_{d,max}$ gradually decreased. In the case of Lig-P and Lig-PN composites, maximum degradation temperature remained constant up to 20 % content. At 30 % Lig-P and Lig-PN content, $T_{d,max}$ decreased but still remained slightly higher than for neat HDPE, Lig-N 30 and Kraft 30.

Regarding the residual mass at 550 °C (Table 3), in all cases, the composites show a progressive increase with the lignin content, with the highest values observed at 30 % wt. filler. Kraft and Lig-N present comparable char residues, while incorporation of phosphorous-containing lignins leads to a significant increase in the residual mass. Interestingly, Lig-PN composites present the highest values among the investigated fillers, reaching approximately 15 % char residue at 30 % additive. This may be attributed to the dehydrating action of phosphoric acid derivatives, indicating the potential of this filler to act as a flame retardant.

Overall, the composites presented good thermal stability mainly because of the antioxidant properties of lignin that shields the polymer network from thermal breakdown, thus providing improved heat-resistance [38]. Although composites containing phosphorus showed slightly lower T_5 values, which could be attributed to the dehydrating action of phosphoric groups, that can catalyse the composite initial

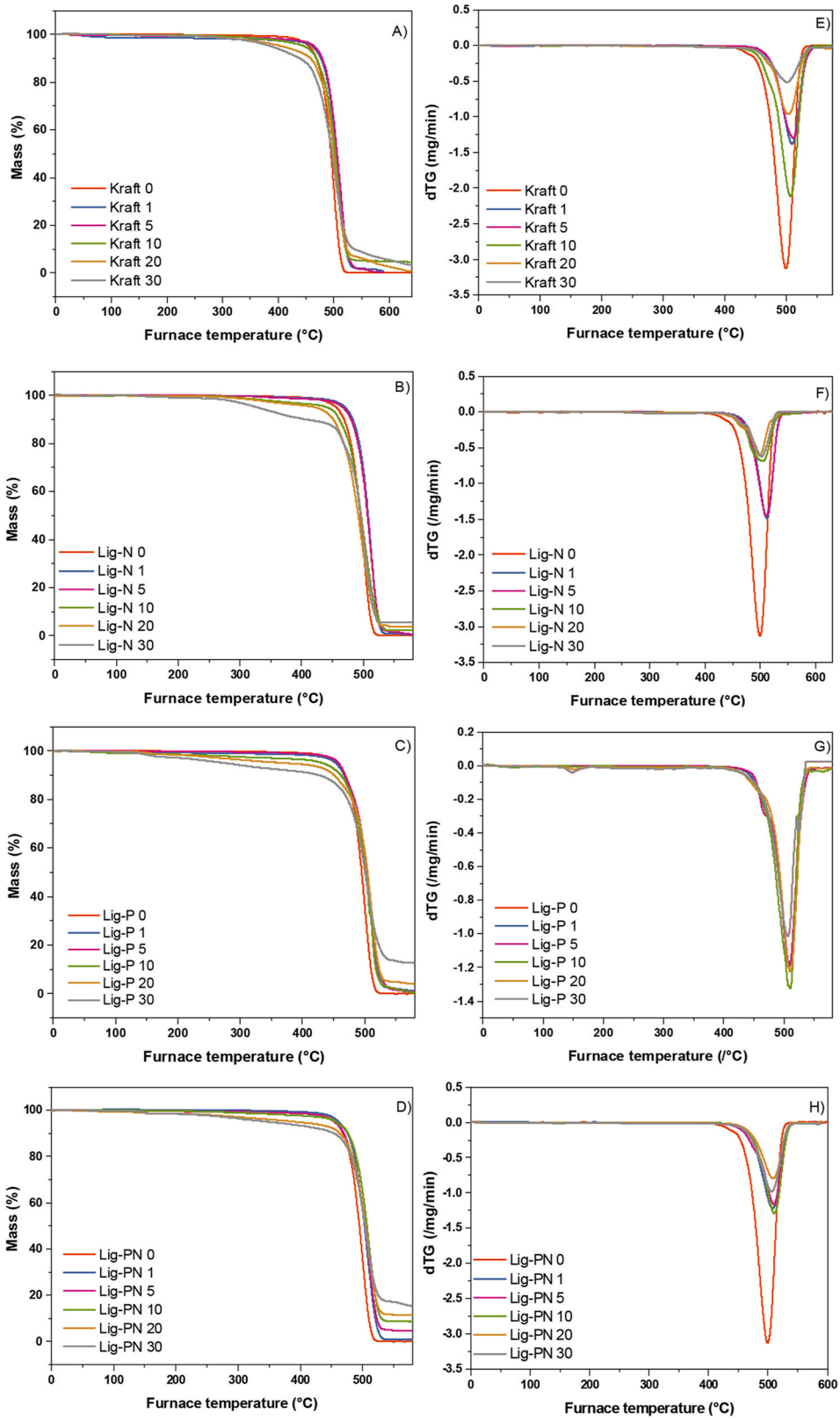

Fig. 15. TGA thermograms of a) Kraft, b) Lig-N, c) Lig-P, d) Lig-PN composites and dTG curves of e) Kraft, f) Lig-N, g) Lig-P, h) Lig-PN.

thermal degradation [20], phosphorus modification proved to be beneficial concerning the thermal stability of HDPE, contributing to an improved $T_{d,max}$. The higher char residue of composites with P-modified lignin is promising regarding flame retardancy [23].

The oxidation induction time (OIT) is a test method used for the evaluation of the stability of polymers at high temperature above the melting point of polymers in oxygen atmosphere. Upon incorporation in a polymeric matrix, an antioxidant additive will typically scavenge the free radicals generated in the oxidation process. Once consumed, oxidation proceeds at a much faster rate, producing an exotherm event

Table 5
Oxidation induction time and flame retardancy results for vertical flame test.

Sample	OIT (min)	Number of drops	Time for ignition (s)	Time of burning (s)
Neat HDPE	14	>10 drops	2	3
Kraft 10	>80	>10 drops	4	60
Kraft 20	>80	>10 drops	5	89
Kraft 30	>80	No dripping	3	145
Lig-N 10	15	>10 drops	6	81
Lig-N 20	26	4-6 drops	6	62
Lig-N 30	30	4-6 drops	4	78
Lig-P 10	47	4-6 drops	5	115
Lig-P 20	49	4-6 drops	5	50
Lig-P 30	45	4 drops	4	40
Lig-PN 10	37	>10 drops	3	69
Lig-PN 20	44	1-2 drops	3	118
Lig-PN 30	60	No dripping	3	107

detectable by DSC. The onset of exotherm is the initiation point of oxidation. Thus, the OIT value is a measure of the thermos-oxidative stability of a composite, while it can also be used to evaluate the effectiveness of an antioxidant [48]. The test results from the HDPE/-lignin composites are presented in Table 5. Kraft lignin is the most effective antioxidant, increasing the OIT from 14 min to more than 80 min. P-containing lignins also improve OIT compared to neat HDPE and Lig-N composites suggesting an effective antioxidant action. These results agree with the evaluation of the antioxidant activity that is discussed in the following paragraphs.

Preliminary vertical flame testing was performed on strips of the composites with 10–30 % additive (Table 5). All composites show lower flammability compared to neat HDPE. On the other hand, clear trends regarding lignin modification or lignin content do not emerge. The composite with 30 % Kraft lignin exhibited the best characteristics with no dripping and a prolonged burning time. Among modified lignins, Lig-PN showed better performance, with overall lower dripping and longer burning times. These encouraging preliminary results will be further complemented with cone calorimetry and limiting oxygen index measurements, to obtain a more comprehensive view of the flame retardant potential of these modified lignins.

3.2.5. *Antioxidant potential and hydrophobicity*

To develop a broader perspective on the potential of P- and N-modified lignins and the properties of the resulting composite materials, antioxidant activity and water contact angle were assessed. Indeed, HDPE and HDPE composites can also find applications as packaging materials and in this case, these are interesting characteristics. Additionally, these characterisation techniques can provided complementary structural insights regarding modified lignins and their composites.

It is apparent that the antioxidant activity of the composites increased with lignin loading (Fig. 16). The highest activity was observed for composites Lig-P and Kraft at 20 & 30 % loading with approximately 10 % and 15–25 % residual DPPH after 4 days, whereas Lig-PN showed the lowest activity. This observation is in agreement with the OIT values that suggested a higher thermo-oxidative stability for the

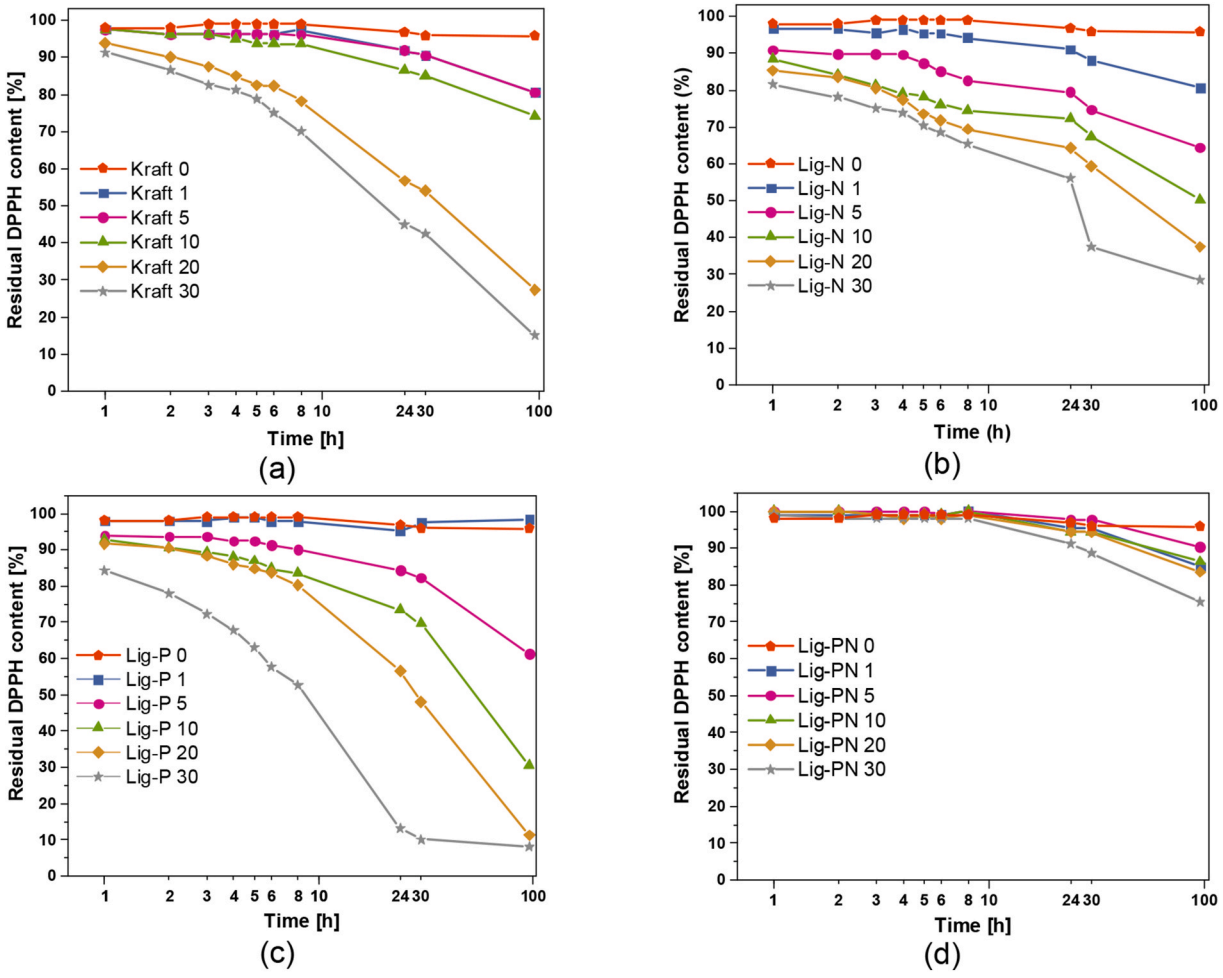

Fig. 16. Antioxidant activity of HDPE composites: Kraft (a), Lig-N (b), Lig-P (c) and Lig-PN (d) at different loadings, measured by monitoring the reduction rate of DPPH radical UV–vis spectroscopy.

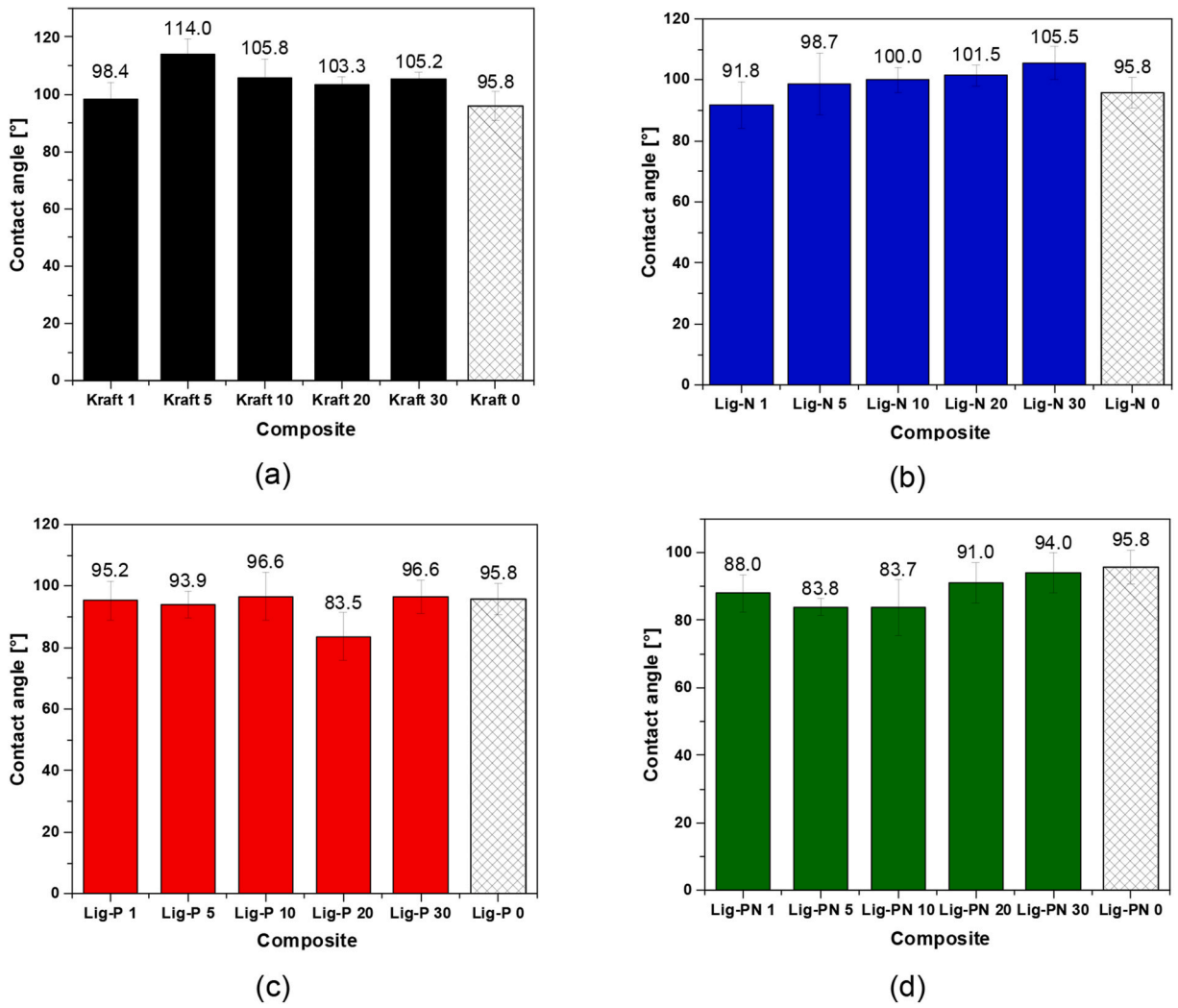

Fig. 17. Contact angle of HDPE composites with different additive loadings. Kraft (a), Lig-N (b), Lig-P (c) and Lig-PN (d).

composites prepared with Kraft lignin and Lig-P. Since antioxidant activity arises from free phenolic hydroxyl groups, the lower antioxidant activity of Lig-PN compared to Lig P, could suggest that the modification with phosphorylamine impacted more phenolic hydroxyl groups, while P_2O_5 phosphorylation affected mainly aliphatic hydroxyl groups. Unfortunately, it was not possible to confirm this observation by ^{31}P NMR spectroscopy.

Finally, contact angle (CA) measurements were performed, Fig. 17. Hydrophobic surfaces are expected to have a CA>90° with poor wetting capability, poorer adhesion and low-surface energy which is typical for most plastics. Hydrophilic surfaces on the other hand, with a CA<90° usually have high surface energy, good wetting capability, better adhesion and is common for glass, metal and ceramic materials. As anticipated, HDPE was found to be hydrophobic (CA = 95.8°). Interestingly, Kraft lignin composites were more hydrophobic than neat HDPE at all loadings. One possible explanation is the loss of hydroxyl groups as water during the heating process of extrusion. The same was true for Lig-N composites, except for the composite with 1 % additive loading (CA = 91.8°). Increasing the Lig-N loading resulted in more hydrophobic composites probably due to the long alkyl chains present in PEI. Lig-P composites on the other hand had a similar contact angle to neat HDPE at all loadings indicating also a similar surface energy, additive loading was observed to have little effect on the contact angle of the composite. Finally, Lig-PN composites are slightly hydrophilic at loadings up to and including 10 % (CA ≤ 88.0°) and hydrophobic for 20 % and 30 % loadings. It should be noted that contact angle measurements are very susceptible to the surface properties and small defaults in composite films could result in some small discrepancies.

4. Conclusions

In the present work, three chemical modifications of lignin, a promising bio-based additive, were investigated to prepare HDPE composites with improved characteristics. To introduce N and P functionalities, lignin backbone was functionalized with polyethyleneimine via a Mannich reaction, or the hydroxyl groups were phosphorylated by phosphorus pentoxide, respectively. To introduce both P and N groups simultaneously, deprotonated OH lignin groups were functionalized by an *in situ* generated phosphoraminochloride intermediate. Infra-red spectroscopy and X-ray photoelectron spectroscopy confirmed the successful modifications. Upon modification, the temperature of maximum weight loss and the char increased compared to Kraft lignin.

The modified lignins were further incorporated in HDPE to prepare environmentally friendly composite materials with added properties. Upon lignin incorporation, the crystallinity of HDPE was slightly disturbed but thermal transitions were not particularly affected. Incorporation of up to 5 % of the lignin-based additives allowed to maintain or improve slightly mechanical behaviour but further increase deteriorated mechanical properties. It is noteworthy that the temperature of maximum weight loss was increased compared to neat HDPE, especially

for the composites prepared with P-containing lignins. Furthermore, lower dripping and flammability were evidenced by preliminary tests for the composite materials compared to neat HDPE. Finally, the composite materials displayed good antioxidant properties, proportional to the content of the lignin-based additive. This good antioxidant potential would support applications in the field of active packaging, although more in-depth studies are necessary.

To conclude, composite materials with interesting properties were obtained, exploiting lignin, an inexpensive, bio-based compound produced as a by-product of the pulping industry. Complementary studies are underway to achieve better understanding of the flame retardancy effect and how it can be further improved.

CRediT authorship contribution statement

Alexander F. Tiniakos: Writing – original draft, Methodology, Investigation, Conceptualization. **Christina Samiotaki:** Writing – original draft, Methodology, Investigation. **Alexandra Zamboulis:** Writing – review & editing, Writing – original draft, Supervision, Project administration, Methodology. **Alexios Grigoropoulos:** Writing – review & editing, Supervision, Methodology, Conceptualization. **Stefania Koutsourea:** Investigation. **Evangelia Tarani:** Writing – original draft, Investigation. **Aikaterini Teknetzi:** Writing – review & editing, Investigation. **George Vourlias:** Writing – review & editing, Supervision. **Alexandros Zoikis Karathanasis:** Writing – review & editing, Supervision, Project administration, Funding acquisition, Conceptualization. **Dimitrios N. Bikiaris:** Writing – review & editing, Supervision, Project administration, Funding acquisition, Conceptualization. **Ioanna Deligkiozi:** Writing – review & editing.

Institutional review board statement

Not applicable.

Funding

This project received funding from the European Union#8217; s Horizon Europe Framework Programme under Grant Agreement No. 101058449 (REDONDO). The views and opinions expressed in this article are, however, those of the author(s) only and do not necessarily reflect those of the European Union or HADEA. Neither the European Union nor the granting authority can be held responsible for them.

Declaration of competing interest

The authors declare that they have no known competing financial interests or personal relationships that could have appeared to influence the work reported in this paper.

Acknowledgments

The authors would like to thank Dr Antonios Anastasiou from the University of Manchester for the TEM imaging, and Dr Martin Sedáček for the flame retardancy measurements. The authors would like to acknowledge the Center of Interdisciplinary Research and Innovation of Aristotle University of Thessaloniki (CIRI-AUTH), Greece, for access to the Large Research Infrastructure and Instrumentation of the Liquid Chromatography and Mass Spectrometry Laboratory at the Center for Research of the Structure of Matter in the School of Chemical Engineering.

Appendix A. Supplementary data

Supplementary data to this article can be found online at https://doi.org/10.1016/j.polymer.2025.129495.

Data availability

Data will be made available on request.

References

[1] Mordor Intelligence, Polyolefin market size & share analysis - Growth trends & forecasts (2025 - 2030), (n.d.). https://www.mordorintelligence.com/industry-reports/polyolefin-market.
[2] Global Growth Insights, High density polyethylene (HDPE) market size, share, growth, and industry analysis by types (naphtha, natural gas, others), by application covered (blow molding, film ad sheet, injection molding, pipe and extrusion, others), regional insights and forecast, (n.d.). https://www.globalgrowthinsights.com/market-reports/high-density-polyethylene-hdpe-market-108754.
[3] L. Hu, T. Stevanovic, D. Rodrigue, Comparative study of polyethylene composites containing industrial lignins, Polym. Polym. Compos. 23 (2015) 369–374, https://doi.org/10.1177/096739111502300602.
[4] M.K. Singh, A.K. Mohanty, M. Misra, Upcycling of waste polyolefins in natural fiber and sustainable filler-based biocomposites: a study on recent developments and future perspectives, Compos. B Eng. 263 (2023) 110852, https://doi.org/10.1016/j.compositesb.2023.110852.
[5] R.R.N. Sailaja, M.V. Deepthi, Mechanical and thermal properties of compatibilized composites of polyethylene and esterified lignin, Mater. Des. 31 (2010) 4369–4379, https://doi.org/10.1016/j.matdes.2010.03.046.
[6] Global lignin market size & outlook, 2024-2030, (n.d.). https://www.grandviewresearch.com/horizon/outlook/lignin-market-size/global (accessed October 24, 2024).
[7] D.S. Bajwa, G. Pourhashem, A.H. Ullah, S.G. Bajwa, A concise review of current lignin production, applications, products and their environment impact, Ind. Crops Prod. 139 (2019) 111526, https://doi.org/10.1016/j.indcrop.2019.111526.
[8] R.J. Khan, C.Y. Lau, J. Guan, C.H. Lam, J. Zhao, Y. Ji, H. Wang, J. Xu, D.J. Lee, S. Y. Leu, Recent advances of lignin valorization techniques toward sustainable aromatics and potential benchmarks to fossil refinery products, Bioresour. Technol. 346 (2022) 126419, https://doi.org/10.1016/j.biortech.2021.126419.
[9] B. Lok, G. Mueller, J. Ganster, J. Erdmann, A. Buettner, P. Denk, Odor and constituent odorants of HDPE–lignin blends of different lignin origin, Polymers (Basel) 14 (2022) 1–22, https://doi.org/10.3390/polym14010206.
[10] K. Komisarz, T.M. Majka, K. Pielichowski, Chemical and physical modification of lignin for green polymeric composite materials, Materials 16 (2023) 16, https://doi.org/10.3390/ma16010016.
[11] O.A.T. Dias, D.R. N, R.C. S, C.S. F, I. C, A.L. Leao, Studies of lignin as reinforcement for plastics composites, Mol. Cryst. Liq. Cryst. 628 (2016) 72–78, https://doi.org/10.1080/15421406.2015.1137677.
[12] E.A. Agustiany, M. Rasyidur Ridho, M. Rahmi DN, E.W. Madyaratri, F. Falah, M.A. R. Lubis, N.N. Solihat, F.A. Syamani, P. Karungamye, A. Sohail, D.S. Nawawi, A. H. Prianto, A.H. Iswanto, M. Ghozali, W.K. Restu, I. Juliana, P. Antov, L. Kristak, W. Fatriasari, A. Fudholi, Recent developments in lignin modification and its application in lignin-based green composites: a review, Polym. Compos. 43 (2022) 4848–4865, https://doi.org/10.1002/pc.26824.
[13] M. Thunga, K. Chen, D. Grewell, M.R. Kessler, Bio-renewable precursor fibers from lignin/polylactide blends for conversion to carbon fibers, Carbon N Y 68 (2014) 159–166, https://doi.org/10.1016/j.carbon.2013.10.075.
[14] J. Guo, X. Chen, J. Wang, Y. He, H. Xie, Q. Zheng, The influence of compatibility on the structure and properties of PLA/Lignin biocomposites by chemical modification, Polymers (Basel) 12 (2020) 56, https://doi.org/10.3390/polym12010056.
[15] P.A. Victor, S.B. Gonçalves, F. Machado, Styrene/Lignin-based polymeric composites obtained through a sequential mass-suspension polymerization process, J. Polym. Environ. 26 (2018) 1755–1774, https://doi.org/10.1007/s10924-017-1078-2.
[16] W. Zhou, C. Fangeng, Z. Hui, J. Wang, Preparation of a polyhydric aminated lignin and its use in the preparation of polyurethane film, J. Wood Chem. Technol. 37 (2017) 323–333, https://doi.org/10.1080/02773813.2017.1299185.
[17] Y. Matsushita, S. Yasuda, Preparation and evaluation of lignosulfonates as a dispersant for gypsum paste from acid hydrolysis lignin, Bioresour. Technol. 96 (2005) 465–470, https://doi.org/10.1016/j.biortech.2004.05.023.
[18] L. Musilová, A. Mráček, A. Kovalcik, P. Smolka, A. Minařík, P. Humpolíček, R. Vícha, P. Ponížil, Hyaluronan hydrogels modified by glycinated kraft lignin: morphology, swelling, viscoelastic properties and biocompatibility, Carbohydr. Polym. 181 (2018) 394–403, https://doi.org/10.1016/j.carbpol.2017.10.048.
[19] J. Liu, H.F. Liu, L. Deng, B. Liao, Q.X. Guo, Improving aging resistance and mechanical properties of waterborne polyurethanes modified by lignin amines, J. Appl. Polym. Sci. 130 (2013) 1736–1742, https://doi.org/10.1002/app.39267.
[20] J.H. Lee, D. Jang, I. Yang, S.M. Jo, S. Lee, Effect of phosphorylated lignin on flame retardancy of polypropylene-based composites, J. Appl. Polym. Sci. 139 (2022) e52519, https://doi.org/10.1002/app.52519.
[21] L. Costes, F. Laoutid, M. Aguedo, A. Richel, S. Brohez, C. Delvosalle, P. Dubois, Phosphorus and nitrogen derivatization as efficient route for improvement of lignin flame retardant action in PLA, Eur. Polym. J. 84 (2016) 652–667, https://doi.org/10.1016/j.eurpolymj.2016.10.003.
[22] L. Liu, M. Qian, P.P. Song, G. Huang, Y. Yu, S. Fu, Fabrication of green lignin-based flame retardants for enhancing the thermal and fire retardancy properties of polypropylene/wood composites, ACS Sustain. Chem. Eng. 4 (2016) 2422–2431, https://doi.org/10.1021/acssuschemeng.6b00112.

[23] Y. Yu, S. Fu, P. Song, X. Luo, Y. Jin, F. Lu, Q. Wu, J. Ye, Functionalized lignin by grafting phosphorus-nitrogen improves the thermal stability and flame retardancy of polypropylene, Polym. Degrad. Stabil. 97 (2012) 541–546, https://doi.org/10.1016/j.polymdegradstab.2012.01.020.
[24] Y. Li, H. Song, L. Qi, G. Zhen, Y. Liang, X. Liu, C. Li, Q. Xie, Modified lignin-based intumescent flame retardant's effect on flame retardancy, mechanical and electrical properties of HDPE material for cable sheathing, Polym. Test. 135 (2024) 108464, https://doi.org/10.1016/j.polymertesting.2024.108464.
[25] B. Prieur, M. Meub, M. Wittemann, R. Klein, S. Bellayer, G. Fontaine, S. Bourbigot, Phosphorylation of lignin to flame retard acrylonitrile butadiene styrene (ABS), Polym. Degrad. Stabil. 127 (2016) 32–43, https://doi.org/10.1016/j.polymdegradstab.2016.01.015.
[26] ASTM D882-18 - standard test method for tensile properties of thin plastic sheeting, (n.d.). https://doi.org/10.1520/D0882-18.
[27] D.S. Argyropoulos, N. Pajer, C. Crestini, Quantitative 31P NMR analysis of lignins and tannins, JoVE J. (2021) e62696, https://doi.org/10.3791/62696.
[28] S.-H. Hong, S.-H. Hwang, Construction, physical properties and foaming behavior of high-content lignin reinforced low-density polyethylene biocomposites, Polymers (Basel) 14 (2022) 2688, https://doi.org/10.3390/polym14132688.
[29] E. Hu, H. Yuan, Y. Du, X. Chen, LDPE and HDPE microplastics differently affect the transport of tetracycline in saturated porous media, Materials 14 (2021) 1–10, https://doi.org/10.3390/ma14071757.
[30] M. Ghozali, E. Triwulandari, A. Haryono, E. Yuanita, Effect of lignin on morphology, biodegradability, mechanical and thermal properties of low linear density polyethylene/lignin biocomposites, IOP Conf. Ser. Mater. Sci. Eng. 223 (2017) 012022, https://doi.org/10.1088/1757-899X/223/1/012022.
[31] S.P. Makri, E. Xanthopoulou, M.A. Valera, A. Mangas, G. Marra, V. Ruiz, S. Koltsakidis, D. Tzetzis, A. Zoikis Karathanasis, I. Deligkiozi, N. Nikolaidis, D. Bikiaris, Z. Terzopoulou, Poly(Lactic acid) composites with lignin and nanolignin synthesized by in situ reactive processing, Polymers (Basel) 15 (2023) 2386, https://doi.org/10.3390/polym15102386.
[32] S.P. Makri, P.A. Klonos, G. Marra, A.Z. Karathanasis, I. Deligkiozi, M.Á. Valera, A. Mangas, N. Nikolaidis, Z. Terzopoulou, A. Kyritsis, D.N. Bikiaris, Structure–property relationships in renewable composites of poly(lactic acid) reinforced by low amounts of micro- and nano-kraft-lignin, Soft Matter 20 (2024) 5014–5027, https://doi.org/10.1039/D4SM00622D.
[33] M. Li, Y. Jia, X. Shen, T. Shen, Z. Tan, W. Zhuang, G. Zhao, C. Zhu, H. Ying, Investigation into lignin modified PBAT/thermoplastic starch composites: thermal, mechanical, rheological and water absorption properties, Ind. Crops Prod. 171 (2021) 113916, https://doi.org/10.1016/j.indcrop.2021.113916.
[34] E. Xanthopoulou, I. Chrysafi, P. Polychronidis, A. Zamboulis, D.N. Bikiaris, Evaluation of eco-friendly hemp-fiber-reinforced recycled HDPE composites, J. Compos. Sci. 7 (2023) 138, https://doi.org/10.3390/jcs7040138.
[35] C. Sukwijit, A. Seubsai, M. Charoenchaitrakool, K. Sudsakorn, C. Niamnuy, S. Roddecha, P. Prapainainar, Production of PLA/cellulose derived from pineapple leaves as bio-degradable mulch film, Int. J. Biol. Macromol. 270 (2024) 132299, https://doi.org/10.1016/j.ijbiomac.2024.132299.
[36] J. Vachon, D. Assad-Alkhateb, L. de Araujo Hsia, J.H. Lora, S. Baumberger, Effect of compatibilizers on polyethylene-eucalyptus lignin blends, J. Appl. Polym. Sci. 140 (2023) e53695, https://doi.org/10.1002/app.53695.
[37] F. Chen, H. Dai, X. Dong, J. Yang, M. Zhong, Physical properties of lignin-based polypropylene blends, Polym. Compos. 32 (2011) 1019–1025, https://doi.org/10.1002/pc.21087.
[38] A. V Maldhure, Jayant D. Ekhe, Effect of modifications of lignin on thermal, structural, and mechanical properties of polypropylene/modified lignin blends, J. Thermoplast. Compos. Mater. 30 (2015) 625–645, https://doi.org/10.1177/0892705715610402.
[39] R. Pucciariello, V. Villani, C. Bonini, M. D'Auria, T. Vetere, Physical properties of straw lignin-based polymer blends, Polymer (Guildf.) 45 (2004) 4159–4169, https://doi.org/10.1016/j.polymer.2004.03.098.
[40] Z. Terzopoulou, E. Xanthopoulou, N. Pardalis, C.P. Pappa, S. Torofias, K. S. Triantafyllidis, D.N. Bikiaris, Synthesis and characterization of poly(lactic acid) composites with organosolv lignin, Molecules 27 (2022) 8143, https://doi.org/10.3390/molecules27238143.
[41] R. Kumar Singla, S.N. Maiti, A.K. Ghosh, Crystallization, morphological, and mechanical response of Poly(Lactic Acid)/Lignin-Based biodegradable composites, Polym. Plast. Technol. Eng. 55 (2016) 475–485, https://doi.org/10.1080/03602559.2015.1098688.
[42] V.G.K. Menta, I. Tahir, A. Abutunis, Effects of blending tobacco lignin with HDPE on thermal and mechanical properties, Materials 15 (2022) 4437, https://doi.org/10.3390/ma15134437.
[43] K. Shi, G. Liu, H. Sun, Y. Weng, Polylactic acid/lignin composites: a review, Polymers (Basel) 15 (2023) 2807, https://doi.org/10.3390/polym15132807.
[44] I. Spiridon, K. Leluk, A.M. Resmerita, R.N. Darie, Evaluation of PLA-lignin bioplastics properties before and after accelerated weathering, Compos. B Eng. 69 (2015) 342–349, https://doi.org/10.1016/j.compositesb.2014.10.006.
[45] I. Grigoriadou, E. Pavlidou, K.M. Paraskevopoulos, Z. Terzopoulou, D.N. Bikiaris, Comparative study of the photochemical stability of HDPE/Ag composites, Polym. Degrad. Stabil. 153 (2018) 23–36, https://doi.org/10.1016/j.polymdegradstab.2018.04.016.
[46] L. Hu, T. Stevanovic, D. Rodrigue, Unmodified and esterified kraft lignin-filled polyethylene composites: compatibilization by free-radical grafting, J. Appl. Polym. Sci. 132 (2015), https://doi.org/10.1002/app.41484.
[47] Y. Guo, S. Zhu, Y. Chen, D. Li, Analysis and identification of the mechanism of damage and fracture of high-filled wood fiber/recycled high-density polyethylene composites, Polymers (Basel) 11 (2019) 170, https://doi.org/10.3390/polym11010170.
[48] A.S. Kabir, Z. Yuan, T. Kuboki, C. (Charles) Xu, De-polymerization of industrial lignins to improve the thermo-oxidative stability of polyolefins, Ind. Crops Prod. 120 (2018) 238–249, https://doi.org/10.1016/j.indcrop.2018.04.072.